Aus dem Institut für Humangenetik

(Prof. Dr. med. B. Wollnik)

der Medizinischen Fakultät der Universität Göttingen

Identification of the molecular role of Pelota protein (PELO) by analysis of conditional Pelo-knockout mice

INAUGURAL-DISSERTATION

zur Erlangung des Doktorgrades

der Medizinischen Fakultät der

Georg-August-Universität zu Göttingen

vorgelegt von

Manar Mohamed Mansour El Kenani

aus

Mansoura, Ägypten

Göttingen 2016

Hiermit erkläre ich, die Dissertation mit dem Titel " **Identification of the molecular role of Pelota protein (PELO) by analysis of conditional Pelo-knockout mice**" eigenständig angefertigt und keine anderen als die von mir angegebenen Quellen und Hilfsmittel verwendet zu haben.

Göttingen, den ……………   ………………………………

                                        (Unterschrift)

Table of contents

List of figures

List of tables

Abbreviations

A.U.	Arbitrary units
AD	Autosomal dominant
AKT	Protein kinase B
AP	Alkaline Phosphatase
AR	Autosomal recessive
atRA	all-trans RA
bFGF	basic Fibroblast Growth Factor
BMP	Bone morphogenetic protein
BrdU	5-Bromo-2′-deoxyuridine
BSA	Bovine Serum Albumine
CDK5	Cyclin dependent kinase 5
CE	Cornified envelope
Dab2	Disabled 2
ddH2O	bi-distilled water
DMEM	Dubecco's Modified Eagle Medium
DNA	Deoxyribonucleic Acid
DNA-PK	DNA-dependent protein kinase
EBs	Embryoid bodies
EDTA	Ethylenediaminetetraacetic Acid
EGF	Epidermal Growth Factor
EGFP	Enhanced Green Fluorescent Protein

EIF3G	Eukaryotic initiation factor type 3G
ELISA	Enzyme Linked Immunosorbent Assay
EM	Electron Microscopy
EPB	Epidermal permeability barrier
eRF1	Eukaryotic release factor 1
ESCs	Embryonic stem cells
et al.	et alii
EtOH	Ethanol
ExEn	Extraembryonic endoderm
FCS	Fetal Calf Serum
Flg	Filaggrin
Foxo1	Forkhead box protein O1
Grhl3	Grainy head–like 3
GSCs	Germline stem cells
GSK3	Glycogen synthase kinase 3
H&E	Hematoxylin-Eosin
HPRT	Hypoxanthine Phosphoribosyltransferase
ICM	Inner cell mass
IGF-1	insulin-like growth factor I
IgG	Immunglobulin G
Intraperitoneally	i.p
IV	Ichthyosis vulgaris
kDa	kilo Dalton
Klf4	Kruppel like factor 4
KO™-SR	KO Serum Replacement

KSR	knock out serum replacement medium
LEF	lymphoid-enhancer binding factor
LIF	Leukemia inhibitory factor
MEF	Mouse Embryonic Fibroblasts
NGD	No-Go decay
NLS	Nuclear localization signal
OCT4	Octamer-binding Transcription Factor 4
PBS	Phosphate Buffered Saline
Pelo	Pelota
PFA	Paraformaldehyde
PI3K	Phosphoinositide 3-kinase
PMSF	Phenylmethylsulfonfluorid
qRT-PCR	quantitative RealTime-PCR
RA	Retinoic acid
RDH	Retinol dehydrogenases
Rnase	Ribonuclease
SC	Stratum corneum
SG	Stratum granulosum
Sox2	Sex Determining Region Y (SRY)-Box 2
SS	Stratum spinosum
SSCs	Spermatogonial stem cells
STRA8	Stimulated by Retinoic Acid Gene 8
TAM	Tamoxifen
TBS	Trisbuffered saline
TCF	T cell factor

TEM	Transmission electron microscopy
Tgase1	Transglutaminase 1
Y kinase	Tyrosine kinase

1. Introduction

1.1 *Pelo* Gene

Pelota (*Pelo*) is a highly conserved gene, which has been firstly identified in Drosophila melanogaster (Castrillon et al.1993). Successive studies have revealed the presence of *Pelo* in the genome of different species from archae to human (Shamsadin et al. 2002). The murine *Pelo* is located on chromosome 13. It consists of three exons, but protein coding sequences are found in the second and third exon. Alignments of the predictive amino acid sequences of PELO from different species showed a high level of sequence conservation. Thus, the protein sequence identity ranged from 55% between mouse and *S. cerevisiae* and 96% between mouse and human.

Structural analysis of PELO protein revealed that it consists of three conserved domains. Two of them (central and C-terminal domains) are RNA-binding domains and express a strong structural similarity to that in the eukaryotic release factor 1 (eRF1). ERF1 has a role in the terminal step of protein translation (Davis and Engebrecht 1998). PELO contains Sm-fold structure, which serves either to recognize mRNA stem loops or to recruit mRNA decay machinery (Tritschler et al. 2007). The N-terminus domain contains a putative nuclear localization signal (NLS) (Shamsadin et al. 2002). However, subcellular localization of transgenic fusion protein EGFP-PELO in *Drosophila* was restricted to cytoplasm (Xi et al. 2005). In fibroblasts of transgenic mouse, the fusion protein EGFP-PELO was localized on the cytoskeleton. Results of subcellular localization of Pelo in murine cells were further confirmed by Western blotting of protein fractions isolated from membrane, nucleus, cytoskeleton and cytoplasm. Immunoblot analysis revealed the presence of Pelo in the membrane and cytoskeleton fractions (Burnicka-Turek et al. 2010).

In an attempt to identify the potential function of Pelo in mammals Burnicka-Turek et al. (2010) has performed yeast two hybrid system to determine the putative interaction partners of PELO in human. By screening of prostate cell line, several cytoskeleton-associated proteins as HAX1 and SEPX and eukaryotic initiation factor type 3G (EIF3G) were identified. The specific interaction of PELO with EIF3G suggests that PELO is involved in protein translation. Further studies have revealed that PELO preferentially bound to epidermal growth factor receptor (HER2/ERBB2) and this binding opposes the direct interaction of HER2 with the p85, a regulatory subunit of PI3K, and thereby attenuating PI3K/AKT signaling in tumor cell lines (Pedersen et al. 2014).

1.2 Biological and molecular role of *Pelo*

The function of PELO has been determined by investigation the effect of *Pelo* mutation on cellular proliferation, differentiation and survival in different species.

1.2.1 *Pelo* and its homolog *Dom34* in yeast

Characterization of mutant *Dom34*, a *Pelo* ortholog in *Saccharomyces cerevisiae,* revealed that the mutation delays the G1 phase of the cell cycle, affects the chromosome segregation, decreases the ability to form pseudohyphae significantly and impairs meiotic division, so that the mutants produce fewer spore compared to that of wild-type controls. Decreased levels of polyribosomal fraction in the extract of mutant *dom34Δ* suggest that the translation of a subset of proteins involved in these processes is specifically affected by Dom34 deficiency (Davis and Engebrecht 1998).

Further characterization revealed that the Dom34 interact with Hsb1 and they are the main components of the RNA quality control mechanism which is known as No-Go decay (NGD).

During translational elongation, mRNAs with stalled ribosomes at stable stem loop structures, rare codons or premature stop codons are targeted by NGD that stimulates the endonucleolytic cleavage of mRNA (Doma and Parker 2006; Graille et al. 2008; Chen et al. 2010). Results of *in vitro* experiments using a reconstituted yeast translation system revealed that Dom34 is involved in ribosomes recycling by binding to the ribosome A site to promote dissociation of ribosome subunits (Shoemaker and Green 2011; Pisareva et al. 2011). Other reports showed that Dom34/Hsb1 complex cause dissociation of the stalled ribosomes at 3´end and is also involved in non-stop decay as well as in decay of non functional 18S rRNA (Cole et al. 2009; Kobayashi et al. 2010; Tsuboi et al. 2012).

1.2.2 *Pelo* deletion in Drosophila impairs the fertility

The functional role of PELO was originally studied in *D. melanogaster*. Mutant male, showed normal progression of the four mitotic divisions during germ cell development, however during the first meiotic division, the cell cycle is arrested between the premeiotic stages G2-M, therefore mutants are sterile. Despite the arrested meiotic division, the resulted *Pelo*-deficient spermatocytes with 4N DNA content continue the germ cell differentiation and form spermatozoa-like cells with head and tail structures. On the contrary, meiotic division is not affected during germ cell development of mutant females (Eberhart and Wasserman 1995). Further study revealed that the balance between self-renewal and differentiation of the gremline stem cells (GSCs) in female mutants is disrupted, resulting in sub-fertility. Results of this study suggest that PELO represses the expression of differentiation-induced genes in GSCs through the activation of bone morphogenetic protein (BMP) signaling and thereby controls its self-renewal (Xi et al. 2005). Recently, it has been shown that PELO deficiency in testis and ovary causes up-regulation of some germline transposones at both transcript and protein levels. These results

suggest that the PELO and its interacting partner HBS1 are required for transposone silencing in germ cells of Drosophila (Yang et al. 2015).

1.2.3 *Pelo* is essential for early embryonic development in mouse

In mammals, *Pelo* is ubiquitously expressed in various tissues during embryonic development and in adult mice (Shamsadin et al. 2002). Adham et al. (2003) showed that targeted deletion of both *Pelo* alleles by homologous recombination in mice results in embryonic lethality at an early post-implantation stage E6.5. Histological analysis of *Pelo*$^{-/-}$ embryos at embryonic days E6.5 and E7.5 revealed the presence of all three germ layers. *In vitro* culture of mutant blastocysts showed the failure of the inner cell mass (ICM) to expand after hatching from the zona pellucida and to give rise to ESCs. These results suggest that Pelo might be responsible for the regulation of the ICM proliferation and differentiation. To circumvent the early embryonic lethality and to study the role of *Pelo* during embryonic development and postnatal life, conditional knockout mice have been generated, and we investigated the effect of *Pelo* deletion on pluripotency and differentiation of embryonic stem cells (ESCs) and spermatogonial stem cells (SSCs) and on murine development during pre- and postnatal life.

Temporal deletion of *Pelo* during early embryonic development revealed that *Pelo*-deficient embryos at 4-cell stage to blastocyst-stage and its ICMs are able to proliferate, but after hatching (E3.5-E4.0) the growth of ICM is arrested. Surprisingly, depletion of Pelo after E5.5 did not affect the proliferation of the ESCs. These results led us to speculate that PELO is neither required for embryonic development till blastocyst stage nor for the ESCs proliferation, but is required for the developmental processes occurring between embryonic days 4.0 and E5.5. Further experiments revealed that Pelo is essential for the extraembryonic endoderm (ExEn) development, which normally occur between E3.5-E4.5 (Nyamsurem et al. 2014).

1.3 *Pelo* in Embryonic stem cell pluripotency and differentiation

Embryonic stem cells can be obtained from the ICM of pre-implanted embryos and have unlimited capacity for self renewal. ESCs are also capable of giving rise to all germ layers and their derivative cell types, which makes them a precious source for tissue replacement and repair (Martin 1981). Understanding the main regulators of ESC pluripotency and differentiation is crucial for improving the somatic cell reprogramming, which have critical therapeutic applications in the regenerative medicine (Thomson et al. 1998).

ESCs maintain pluripotency by multiple regulators in the form of transcription factors, among them Oct4, Sox2, and Nanog, as well as leukemia inhibitory factor (LIF), BMP and Wnt/ β-catenin signaling pathways. Involvement of PI3K/AKT, Foxo1 and VitaminA/Retinol signalings in the regulation of stemness has been recently proposed (Zhang et al. 2011; Khillan 2014). Recent studies have enabled the construction of regulatory networks between these signaling pathways in ESCs that provide a foundation for understanding ESC self- renewal and differentiation (Lee et al. 2009).

To determine pluripotent potential of *Pelo*-null ESCs and the cause of impaired ExEn development, ESCs were isolated from $Pelo^{F/-}$ blastocysts and $Pelo^F$ allele was recombined ($Pelo^\Delta$) by treatment of $Pelo^{F/-}$ ESCs with Tamoxifen. The differentiation potential of *Pelo*-null ESCs was investigated in embryoid bodies (EBs) and in teratoma assay. Mutant ESCs exhibited infinite proliferation capacity in culture, however they displayed slightly lower growth rate compared to control ESCs. Despite *Pelo*-null ESCs have the capacity to differentiate to all three germ layers in vivo teratoma assay, mutant ESCs were not able to differentiate to ExEn in EBs. Analysis of expression profile of genes, which are expressed at different time points of EXEn development, revealed that the development of ExEn was initiated in *Pelo*-null EBs, but could

not be maintained to the late stages of EB formation. Further experiment revealed that retinoic acid (RA) rescue the development of ExEn in mutant EBs. Molecular analysis showed that the decreased activity of BMP signaling was the underlying cause for the impaired differentiation of ExEn in Pelo-deficient EBs (Nyamsurem et al. 2014).

1.4 *Pelo* in Spermatogonial stem cells development

The first wave of spermatogenesis arises from the gonocytes that are the precursors of spermatogonial stem cells (SSCs), whereas the subsequent waves are directly derived from SSCs (Yoshida et al. 2006; Raju et al. 2015). Maintenance of male germ cell production throughout the life time of an individual is the result of tightly controlled balance between SSC self-renewal and differentiation (Oatley et al. 2006; Raju et al. 2015).

To determine whether PELO deficiency affects the self-renewal and differentiation of germ stem cells, we have deleted *Pelo* during embryonic and adult life. We found that deletion of *Pelo* in adult mice resulted in a complete loss of whole male germ cell lineages after 45 days of deletion. Further analyses revealed that the Pelo is required for maintenance of spermatogonial stem cells, but dispensable for the development of later stages of spermatogenesis. Depletion of *Pelo* during embryonic development showed that Pelo is not essential for maintaining the embryonic gonocytes, but is essential for transition of the gonocytes to SSC (Raju et al. 2015). Molecular analysis suggested that Pelo negatively regulates the PI3K/AKT signaling pathway. The enhanced activity of PI3K/AKT and subsequent Foxo1 inhibition are responsible for the impaired development of SSCs in *Pelo*-null testes.

1.5 Epidermal homeostasis

Skin is the largest organ in the body, composed of three layers called the epidermis, the dermis, and the hypodermis. The epidermis, the outer layer of the skin, serves as the first physical barrier that protects the body from fluid loss and entry of toxic and pathogenic agents. The dermis is the second skin layer contains nerve endings, sweat and oil glands, hair follicles, blood vessels and nerves. The hypodermis is just below the dermis, and consists of fat. In mice, the development of the epidermal barrier is initiated at embryonic day 16.5 (E16.5) and must be accomplished before the end of gestation (Hardman et al. 1998). Disruption or delay in the acquisition of the epidermal barrier is known to result in neonatal lethality (Segre 2006).

Barrier function is conferred by the outer layer of epidermis, the stratum corneum, as it provides a rigid but flexible support to terminally differentiated keratinocytes in the cornified layer (Kalinin et al. 2002). The epidermal barrier is maintained by a balance between proliferation of self-renewing stem cells located in the basal layer and differentiation of their daughter cells (Blanpain and Fuchs 2006). Keratinocyte is the most abundant cell type in the epidermis, which synthesizes the major structural components of the epidermal barrier through a programmed process of differentiation. Basal keratinocytes arise at the innermost layer of the epidermis, after cell division, some progeny remain in the basal layer as stem cells and express specific keratin proteins, K5 and K14, while others migrate into the upper epidermal layers (Fuchs 2007).
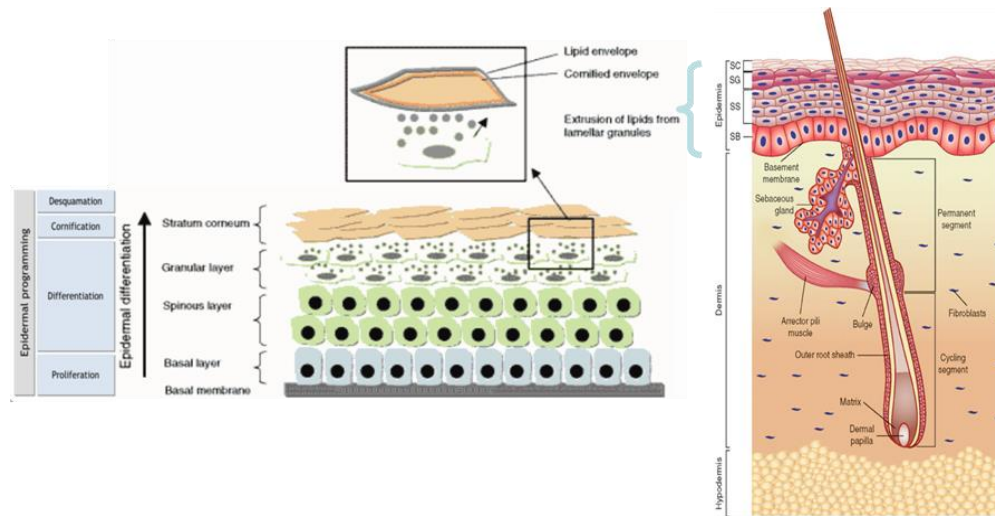
Figure 1. Schematic diagram of the skin architecture. Skin is characterized by two main components, epidermis and dermis separated by a basement membrane. The epidermis is constituted by a lower basal layer which contains a quiescent population of undifferentiated basal cells reserved for regeneration, they progressively differentiate in to the spinous layer, granular layer, and finally the outermost cornified layer (envelope), which is responsible for the vital barrier function of the skin (Adapted from Hoffjan and Stemmler 2007).

During migration the cells change dramatically both biochemically and morphologically they differentiate to suprabasal cells expressing a different set of keratin proteins, K1 and K10, then granular cells expressing markers of late differentiation, such as loricrin, and finally, become flattened enucleated cells of the stratum corneum (SC). Besides the loss of the nucleus and other organelles, the aggregation of keratin intermediate filaments (IF) into macrofibrils and the formation of a cornified cell envelope (CE) are the major structural changes that occur during the differentiation of granular to cornified cells. Filaggrin (Flg), a protein associated with late epidermal differentiation, promotes the assembly of keratin IF to form macrofibrils in the cornified cells (Irvine et al. 2011). Filaggrin is synthesized as a high molecular weight precursor protein called profilaggrin that consists of tandem filaggrin repeats and is stored in keratohyalin granules of granular cells as highly phosphorylated proteins (Sandilands et al. 2009). Profilaggrin is dephosphorylated and proteolytically cleaved into filaggrin monomers that are released into

the lower layer of the SC. Mutations in the *Filaggrin* gene or genes encoding proteins that regulate the post-translational modification of profilaggrin and its processing to mature filaggrin lead to disruption of the epidermal barrier and development of skin disorders (Fallon et al. 2009).
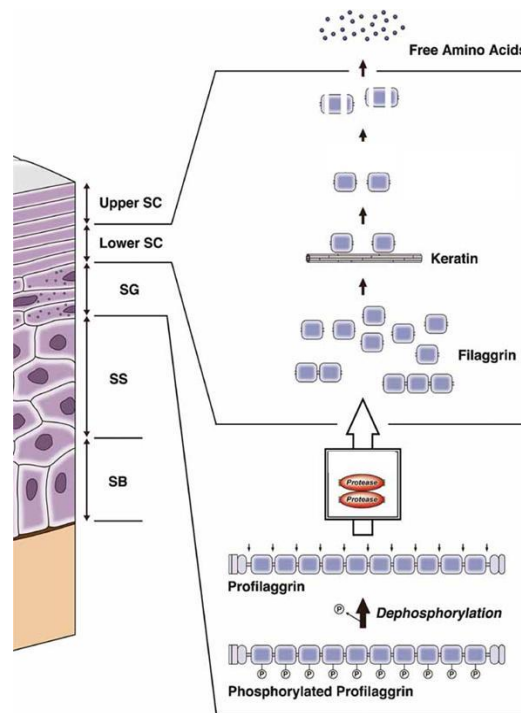
Figure 2. Schematic representation of the profilaggrin processing. Within the granular layer, profilaggrin is stored as a highly phosphorylated, inactive and insoluble form within keratohyalin granules. Profilaggrin is dephosphorylated in the upper most SG. The linker sequence that connects each filaggrin monomer is then cleaved to produce filaggrin intermediates (2DI and 3DI). Further proteolysis occurs and the released filaggrin monomers bind directly to keratin filaments, causing their collapse into thickened and aggregated keratin filaments. In the upper SC filaggrin is released from keratin and further degraded to form free amino acids, which act as a natural moisturising factor (Adapted from Matsui et al. 2011).

Several signaling pathways are involved in mammalian skin barrier development. The role of PI3k/Akt signaling during epidermal barrier acquisition has been recently studied. AKT is a Ser/Thr kinase and downstream mediator of the phosphatidylinositol 3-kinase pathway regulating cell survival, differentiation and growth factor responsiveness. Activation of AKT is antagonized by the PTEN, which dephosphorylates PIP3 and thereby inhibits PI3K/AKT-

mediated survival signaling (Leslie and Downe 2004). Peng et al. (2003) showed that mice lacking both AKT1 and AKT2 die postnatally, probably due to lack of epidermal barrier function. Additionally O'Shaughnessy et al. (2009) reported that epidermal barrier acquisition in late embryonic development is accompanied of AKT activation.

The BMP pathway has a role in skin development and postnatal skin remodeling. BMP ligands and receptors are differentially expressed in the embryonic epidermis (Botchkarev and Sharov 2004). BMPs function by binding type 1 (BMPR1A and BMPR1B) and type 2 (BMPR2) transmembrane serine/threonine kinase receptors, resulting in phosphorylation of the intracellular proteins Smad 1, 5, and 8. Disruption of BMP signaling has been implicated in an array of skin disorders (Kan et al. 2011). However, still limited information is available regarding BMP signaling in epidermis development and homeostasis. Moreover previous reports have suggested that other kinase pathways participate in BMP signaling, including the c-Jun N-terminal kinase, phosphatidylinositol 3-kinase (PI3K) and Wnt signaling pathways (Lee et al. 2009).

1.6 Aim of the study

I.   The first aim of this study was to determine whether the impaired development of the epidermal barrier is the reason for neonatal lethality in *Pelo*-deficient mice and to identify the molecular causes for the disrupted function of epidermal permeability barrier (EPB).

Experimental approaches devised for this study can be summarized as follows:

➢ To determine the cause of neonatal lethality, we temporally deleted *Pelo* at different time-points of embryonic development. To investigate the cause of the epidermal barrier defect observed in mutant embryos, we analyze the differentiation and proliferation status in the skin of $Pelo^{\Delta/\Delta}$ embryos starting from E 15.5 till E18.5 by immunohistological

analysis. To address whether altered distribution of filaggrin in E18.5 $Pelo^{\Delta/\Delta}$ skin is due to defect in filaggrin processing, protein blot analysis was performed.

➢ To determine whether the failure of epidermal barrier formation in *Pelo*-null epidermis is associated with altered activity of PI3K/AKT and BMP signaling, we determined the activity and crosstalk between both signaling pathways in organotypic culture and studied the effect of PI3K/AKT- and BMP-inhibitors on the formation of epidermal barrier.

➢ To determine the consequence of *Pelo* deficiency on epidermal barrier of adult, we performed immunohistological and molecular analyses on skin of mutant and control mice.

II. The second aim was to study the impaired differentiation of *Pelo*-deficient ESCs. For this study, the following experiments were designed:

➢ To check whether the impaired differentiation of mutant ESCs is only occurring during the development of EBs, we studied the differentiation efficiency of $Pelo^{\Delta/-}$ ESCs and the effect of retinoic acid on the induction of $Pelo^{\Delta/-}$ ESCs differentiation as well as the underlying molecular mechanism.

➢ Study the consequences of Pelo deficiency on the activity of PI3K/AKT and Wnt signal pathways in ESCs.

2. Materials and Methods

2.1 Materials

2.1.1 Mice

Pelo^{F/F} Cre ERT2 mice used in this study were generated in the Institute of Human Genetics, University of Göttingen (Nyamsuren et al. 2014).

2.1.2 Antibodies

List of the antibodies used in immunohistochemical analysis with the providing supplier and the working dilution.

Antibody	Provider	Dilution
Alexa Fluor 488 conjugated IgG (rabbit)	Life Technologies, Darmstadt	1:250
Anti-BrdU antibody (rat)	Abcam, Cambridge, UK	1:500
Anti-Filaggrin (rabbit)	Covance,USA; PRB-417P	1:100
Anti-K10 (mouse)	Covance, USA; MMS-159S	1:100
Anti-K14 (rabbit)	Covance, USA; PRB-155P	1:100
anti-Loricrin (rabbit)	Covance, USA; PRB-145P	1:100
Cy3-conjugated anti-mouse IgG antibody	Sigma-Aldrich, Deisenhofen	1:250

List of the antibodies used in western blot analysis with the providing supplier and the working dilution.

Antibody	Provider	Dilution
anti-DAB2 (mouse)	BD Transduction Lab, Heidelberg	1:2000
anti-Filaggrin (rabbit)	Covance, USA	1:5000
anti-Foxo1 (rabbit)	Cell Signaling, USA	1:2000
anti-Oct4 (mouse)	Abcam,Cambridge, UK	1:2000
anti-pAKT(rabbit)	Cell Signaling, USA	1:2000
anti-Pelota (rabbit)	Institute of Human Genetics, Göttingen	1:10,000
anti-pSMAD1/5 (rabbit)	Cell Signaling, USA	1:2000
anti-total AKT(rabbit)	Cell Signaling, USA	1:5000
anti-α-tubulin (mouse)	Sigma-Aldrich, Deisenhofen	1:5000
secondary peroxidase-conjugated antibody (mouse /rabbit)	Sigma-Aldrich, Deisenhofen	1:10,000

List of the antibodies used in ELISA.

Antibody	Provider
anti-mouse IgE	Southern Biotech, USA; 0114-01
anti-mouse IgE (goat)	Southern Biotech, USA; 1110-01
HRP-conjugated anti-mouse IgE (goat)	Southern Biotech, USA; 1110-05

2.1.3 Chemicals

List of the chemicals used in this study.

Name	Manufacturer
1 kb DNA plus Ladder	Invitrogen, Karlsruhe
2,2'-azino-bis (3-ethylbenzothiazoline-6-sulfonic acid)	Sigma-Aldrich, Deisenhofen

2-Mercaptoethanol	Gibco, Eggenstein
Beetle –juice small kit	PJK GmbH, Kleinbilttersdorf
Bovine Serum Albumine (BSA)	Serva, Heidelberg
BrdU (5-Bromo-2′-deoxyuridine)	Sigma-Aldrich, Deisenhofen
Chemiluminescent Substrate	Pierce, Rockford, IL
DAPI	Sigma-Aldrich, Deisenhofen
Dispase	Sigma-Aldrich, Deisenhofen
Dithiothreitol	Sigma-Aldrich, Deisenhofen
dNTPs	Invitrogen, Karlsruhe
EDTA	ICN Biomedicals, Eschwege
Eosin	Sigma-Aldrich, Deisenhofen
Ethanol	Baker, Deventer, NL
Ethidium bromide	Sigma-Aldrich, Deisenhofen
Eukitt-quick hardening mounting medium	Fluka, Neu Ulm
Glutaraldehyde	Sigma-Aldrich, Deisenhofen
Goat serum	PAN-Systems, Nürnberg
Hematoxylin	Sigma-Aldrich, Deisenhofen
Milk powder	Roth, Karlsruhe
Nitrocellulose membranes	Amersham Pharmacia Biotech
NuPAGE MOPS/MES SDS running buffer	Invitrogen, Karlsruhe
NuPAGE Novex Bis-Tris 4-12% Gel	Invitrogen, Karlsruhe
Paraffin	Carl Roth, Karlsruhe
Paraformaldehyde	Sigma-Aldrich, Deisenhofen
Penicillin/Streptomycin	PAN-Systems, Nürnberg
Phosphate buffered saline (PBS)	PAN-Systems, Nürnberg
PMSF	Sigma-Aldrich, Deisenhofen
Protease inhibitor cocktail	Roche, Mannheim
Proteinase K	Carl Roth, Karlsruhe
Renilla Glow –Juice Big kit	PJK GmbH, Kleinbilttersdorf
RIPA buffer	Millipore, Darmstadt
RNase	Sigma-Aldrich, Deisenhofen
SDS	Serva, Heidelberg
SeeBlue Plus2 Pre-Stained Standard	Invitrogen, Karlsruhe
Sodium citrate	Merck, Darmstadt
SuperScript II	Invitrogen, Karlsruhe
SYBR Green	Qiagen, Hilden
Tamoxifen	Sigma-Aldrich , Deisenhofen
Toulidine blue	Sigma-Aldrich, Deisenhofen
Tris base	Sigma-Aldrich, Deisenhofen

TRIzol	Life Technologies, Darmstadt
Tween® 20	Carl Roth, Karlsruhe
Xylene	Carl Roth, Karlsruhe

2.1.4 Cell culture mediums and chemicals

List of the cell culture mediums and chemicals used in cell culture.

Name	Manufacturer
DMEM	Gibco, Eggenstein
Gelatine	Sigma-Aldrich, Deisenhofen
Hydrocortisone	Life Technologies, Darmstadt
Insulin	Life Technologies, Darmstadt
KnockOut™ Serum Replacement	Gibco, Eggenstein
Leukocyte Alkaline Phosphatase Kit	Sigma-Aldrich, Deisenhofen
L-Glutamine	Gibco, Eggenstein
LIF	Millipore, Billerica, USA
Lipofectamine 2000 TM	Invitrogen, Karlsruhe
Lucifer Yellow	Sigma-Aldrich, Deisenhofen
LY-294002	Sigma-Aldrich, Deisenhofen
Mitomycin C	Sigma-Aldrich, Deisenhofen
Noggin	Life Technologies, Darmstadt
Opti-MEM® I + GlutaMAX TM I	Gibco, Eggenstein
Williams Medium E	Life Technologies, Darmstadt

2.1.5 Primers

List of the primers used in this study for genotyping PCR and reverse transcription polymerase chain reaction (RT-PCR) with the sequence.

Primer	Forward	Reverse
Tgm1	TGTCACCCTCACCAACGTC	GACTGTCTCATTACCCCCGA
Grhl3	AGCCAACCAGAGACGGATC	TGGAAGCTCACAGGGTCATT
KlF4	AACATGCCCGGACTTACAAA	TTCAAGGGAATCCTGGTCTTC
IL4	TCTCGAATGTACCAGGAGCC	GGTGTTCTTCGTTGCTGTGA

TSLP	CCAGGCTACCCTGAAATCGA	TCTGGAGATTGCATGAAGGA
PELO	AACTCGAGACAAGCTCGTCG GTCTGAGTG	AACTCGAGGGGACGAAACTATTA ACTGCCAGTC
F1	TGAGCCCAGACTGTACGTGAC	
R1		AACGTCAAAGGAGGCGGTCAG
R2		CCACTTGTGTAGCGCCAAGTG
HPRT	AGCCCCAAAATGGTTAAGGTTGC	TTGCAGATTCAACTTGCGCTCAT
Stra8	TCACAGCCTCAAAGTGGCAGG	GCAACAGAGTGGAGGAGGAGT

2.1.6 Buffers and cell culture mediums

List of the buffers and mediums used in this study.

Buffer	Composition
Blocking Solution (Western Blotting)	100 mM Tris-HCl, pH 7.5 0.1 % Tween20 5% milk powder in ddH2O
ESC medium	DMEM 20% FCS 0.1 mM NEAA 1 mM Sodium Pyruvate 0.2 mM 2-ME 2 mM L-Glutamine 1 mM P/S
KO ESC medium	DMEM 20% Knockout^{TM} serum replacement 0.1 mM NEAA 1 mM Sodium Pyruvate 0.2 mM 2-ME 2 mM L-Glutamine 1 mM P/S 1000 U/ml LIF
Protein Lysis Buffer (Western Blotting)	1 mM PMSF (in isopropanol) Protease Inhibitor Cocktai Tablets 1× RIPA lysis buffer

Transfer Buffer (Western Blotting)	25 mM Tris-HCl, pH 8.3 150 mM Glycin 20% Methanol
Washing Solution (Western Blotting)	100 mM Tris-HCl, pH 7.5 0.1 % Tween20 2% milk powder in ddH2O
Cornified envelope buffer	20 mM Tris-HCl (pH 7.5) 5 mM EDTA 10 mM dithiotreitol 2% SDS

2.1.7 Equipments

List of the equipment used in this study

Equipment	Manufacturer
Incubator for paraffin (60°C)	MWG Biotech, Ebersbach
Centrifuge 5415D	Eppendorf, Hamburg
Thermomixer 5436	Eppendorf, Hamburg
Nanodrop 2000	Thermo Scientific, Schwerte
pH Meter	Sartorius, Göttingen
Semi-Dry-Blot Fast Blot	Biometra, Göttingen
Thermocycler (Advanced Primus 96)	peqlab, Erlangen
Microscopes • Confocal laser scanning microscope • Fluorescence microscope BX60 • Inverse microscope IX71	Olympus, Hamburg
7900HT Fast Real-Time PCR System	Applied Biosystems Deutschland
Microplate reader	Powerwave 340, BioTek Instruments
Cell culture plates	Greiner Bio-one, Frickenhausen

2.2 Methods

2.2.1 Temporal deletion of *Pelo* in mice

To inactivate *Pelo* before the development of the skin barrier, pregnant *Pelo*$^{F/F}$ *Cre ERT2* and control *Pelo*$^{F/F}$ mice were injected intraperitonally (i.p) with tamoxifen (TAM) at gestational days 13.5 and 14.5. To delete *Pelo* in 8-week-old *Pelo*$^{F/F}$ *Cre ERT2, Pelo*$^{F/+}$*CreERT2* and *Pelo*$^{F/F}$ mice, animals were i.p injected with 1 mg Tam for 5 consecutive days. For the local depletion of PELO protein in the skin of adult mice *Pelo*$^{F/F}$ and *Pelo*$^{F/F}$ *Cre ERT2* mice were topically treated with 100 μl of 4-hydroxytamoxifen (4-OHT) dissolved in ethanol at a concentration of 1 mg/ml on 1 cm^2 of tail skin for 5 consecutive days. Skin samples were prepared from Tam-treated mutant *Pelo*$^{Δ/Δ}$*CreERT* and control *Pelo*$^{F/F}$ embryos at E15.5, E16.5, E17.5 and E18.5 and from adult animals after 60-90 days of the last day of Tam injection.

All experiments involving mice were performed according to protocols authorized by the Institutional Animal Care and Use Committee of the University of Göttingen. (AZ: 33.9-42502-04-14/1487).

2.2.2 Histological and immunohistochemical analysis

Skin samples were dissected from freshly sacrificed embryos and adult mice, fixed in 4% paraformaldehyde (PFA) at 4°C overnight, dehydrated through a graded ethanol series, embedded in paraffin and cut into 5 μm sections. Sections were stained with hematoxylin and Eosin (H&E), toluidine blue or subjected to immunofluorescent analysis. Toulidine blue staining was performed to detect mast cells and the number of mast cells was counted under the microscope at x100 magnification from 4-5 fields for each skin sample from 3-4 different mice for genotype.

For immunofluorescent staining, skin sections were rehydrated, boiled for 10 min in 10 mM sodium citrate antigen retrieval buffer and blocked for 1 h with 10% goat serum in Trisbuffered saline at pH 7.4 (TBS). The tissue sections were incubated overnight at 4°C in the primary antibody. After washing with TBS, tissue sections were incubated with the secondary antibody 2 h at room temperature. DAPI was used for nuclear staining. Microscopic images were taken using either an A1 or A1R Nikon confocal microscope. Epidermal layer quantification was performed using Fiji Image J software. For epidermal layer quantification experiments, sampling areas for measurement were taken from the basal layer to the differentiated layer defined by expression of specific markers. An unpaired t-test was used for statistical comparison between $Pelo^{F/F}$ and $Pelo^{\Delta/\Delta}$ epidermal layers.

2.2.3 Proliferation assay

Cell proliferation was measured by i.p injection of pregnant mice gestational day 18.5 with 50 mg/kg BrdU and the embryos were sacrificed 2 h later. Skin sections prepared as described above were incubated with anti-BrdU antibody and anti-K14. The numbers of epidermal BrdU positive nuclei relative to total number of k14 positive cells in the basal layer were counted at x 20 magnification in 5-7 microscopic fields per skin sample from 3-4 different mice per genotype.

2.2.4 Skin permeability staining

An in situ dye permeability assay with toluidine blue was performed using $Pelo^{F/F}$ and $Pelo^{\Delta/\Delta}$ embryos at E18.5 as previously described (Hardman et al. 1998).

2.2.5 Embryonic epidermal explant culture

Organotypic culture of embryonic skin was performed as described previously (O'Shaughnessy et al. 2009). Briefly, pregnant female mice were i.p injected with Tam at gestational day 13.5 and 14.5

as described previously. Back skin was dissected from embryos at E15.5, rinsed in sterile PBS and cultured dermis side down at the air-liquid interface for 48 hours. Explants were cultured in Williams Medium E supplemented with 10 µg/ml insulin, 10 ng/ml hydrocortisone, 2 mM L-glutamine, 100 IU/l penicillin, 100 mg/l streptomycin. To study the effect of down-regulation of AKT and BMP signaling pathways on skin development, AKT inhibitor LY-294002 (150 µmol/l) or BMP inhibitor Noggin (400 ng/ml) was added to the culture 24 h prior to collection of the explants. Cultured explants were divided into portions, one of which was fixed in 4% PFA for immunostaining and the other was used for protein extraction. For analyzing barrier function acquisition in skin explants, 30 µl of 1 mM Lucifer Yellow was applied to the skin samples and incubated at 37°C for 1 hour before fixation with 4% PFA.

2.2.6 Protein extraction and Immunoblotting

Epidermal sheets were detached from the dermis by digestion with dispase at 4°C overnight. For protein extraction, the epidermis was homogenized in cold RIPA buffer supplemented with protease inhibitor cocktail and 1 mM PMSF. Homogenates were sonicated and centrifuged at 12000 g for 20 min at 4°C.

Protein lysates were resolved on 4–12% SDS-PAGE and transferred onto nitrocellulose membranes. Membranes were blocked for 1 h with 5% non-fat milk in 0.1% Tween 20 in TBS. Blots were probed at 4°C overnight with primary antibody, followed by incubation with a secondary peroxidase-conjugated antibody. Signals were detected using a chemiluminescent kit and an AlphaView image analyzer. Signals were quantified by using AlphaView software; Version: 3.2.0 (Cell Biosciences Inc, Santa Clara, CA).

2.2.7 Cornified envelope preparation

Isolated epidermis from E18.5 embryos was cut into 5 mm^2 pieces and boiled for 20 min in cornified envelope buffer. Cornified envelopes (CEs) were centrifuged at 6000 *g*, washed in CE buffer containing 0.2% SDS, pelleted, and resuspended in CE buffer for microscopic analysis. At least 200 CEs were counted for each of the three mutant and control embryos.

2.2.8 RNA preparation and real time PCR

Total RNAs were isolated using TRIzol reagent, followed by treatment with RNase free DNase for 1 h at 37°C and reverse transcribed using the Superscript II first strand kit. Quantitative RT-PCR (qRT-PCR) was performed in triplicate on an ABI Prism 7900HT sequence detection system using QuantiTect SYBR Green PCR Master mix, following the manufacturer's instructions. RNA expression levels were normalized to hypoxanthine guanine phosphoribosyl transferase (*Hprt*).The primer sequences are listed in 2.1.5.

2.2.9 Transmission electron microscopy (TEM)

Skin samples were fixed in 2.5% glutaraldehyde in PBS, pH 7.4 for 4 h and embedded in Epon resin.TEM was performed on ultra-thin sections (100 nm) stained with uranyl acetate and counterstained with lead citrate. Images were taken with a Philips CM10 instrument at 80 kV.

2.2.10 Enzyme-linked immunosorbent assay (ELISA) for IgE

Ninty- six well ELISA plates were coated with an immunoglobulin isotype-specific antibody to mouse IgE in 50 mM carbonate buffer, pH 9.6. Upon incubation for 3 h at 37°C, plates were blocked with 1% BSA in PBS for 1 h at 37°C. Serum samples were diluted from 1:20 to 1:1280 in duplicate and incubated at 4°C overnight. To calculate immunoglobulin concentrations,

purified mouse IgE was diluted from 500 ng/ml to 7.8 ng/ml on each plate as a standard. After washing, plates were incubated with a HRP-conjugated goat-anti-mouse IgE for 2 h at 37°C and washed again. For colorimetric detection 2,2'-azino-bis (3-ethylbenzothiazoline-6-sulphonic acid) was used as a substrate. Absorbance was measured at 450 nm in a microplate reader.

2.2.11 Cell culture

ESCs were maintained on Mitomycin C-treated MEF feeder layers in LIF-supplemented medium, cells were incubated at 37°C with 5% CO_2 in a humidified incubator. For mono-layer differentiation, ESCs were plated on gelatin coated plates at a density of 1000 cell per 1 cm^2 in DMEM medium supplemented with 20% Knockout^{TM} serum replacement, in absence of LIF.

2.2.12 Alkaline Phosphatase Staining

Cells were washed with PBS, fixed for 30 sec. with fixation solution (Sigma) washed with PBS, then Cytochemical staining for alkaline phosphatase (AP) activity was performed using a Leukocyte Alkaline Phosphatase Kit according to the manufacturer's instructions.

2.2.13 Transfections, Luciferase reporter assays

Cells were plated in 24-well plates at a density of 5×10^2 per well. Transient transfection was done using lipofectamine reagent and OPTIMEM I medium according to the supplier's instructions with 5 µg of total TCF/LEF luciferase reporter (TOP) and its negative control (FOP) plasmids with renilla plasmid as an internal control. After 24-36 h of transfection, luciferase levels were assessed using Dual reagent as described in the kit instructions.

2.2.14 Statistical analyses

Data were expressed as mean ± SEM. Differences among groups were tested by the Student's *t* test or two-way ANOVA test when appropriate. A *P* value < 0.05 was considered to be significant.

3. Results

To investigate the molecular role of Pelota, Nyamsuren et al. (2014) generated *Pelo* conditional knockout mouse model. The effect of conditional *Pelo* ablation on the proliferation and differentiation of embryonic and spermatogonial stem cells was analyzed (Nyamsuren et al. 2014; Raju et al. 2015). In the first part of this study we have determined the role of *Pelo* in the epidermal barrier development.

3.1 Role of *Pelo* in epidermal barrier acquisition

During mouse embryogenesis, the development of EPB is initiated at embryonic day 16.5 (E16.5) and accomplished before the end of gestation (Hardman et al. 1998). Several lines of evidence demonstrated that disruption or delay in the formation of the epidermal barrier results in neonatal lethality (Plamer et al. 2006; Segre 2006).

3.1.1 Deletion of *Pelo* prior to skin barrier formation causes neonatal lethality

To determine the effect of temporal *Pelo* deletion on embryonic and postnatal development, pregnant $Pelo^{F/F}CreERT2^{+/-}$ females, which were intercrossed with $Pelo^{F/F}CreERT2^{+/-}$ males, were i.p injected with TAM at different gestational days, E13.5 and E14.5 or E17.5 and E 18.5. No progeny were found on the expected delivery days from pregnant females, which were i.p injected with TAM at gestational days 13.5 and 14.5. In contrast, pregnant females treated with TAM at E17.5 of gestation gave litters, but all mutant pups died between P7 and P14 (Figure 3a, b). These results suggested that the neonatal lethality may be due to defect in the function of EPB.
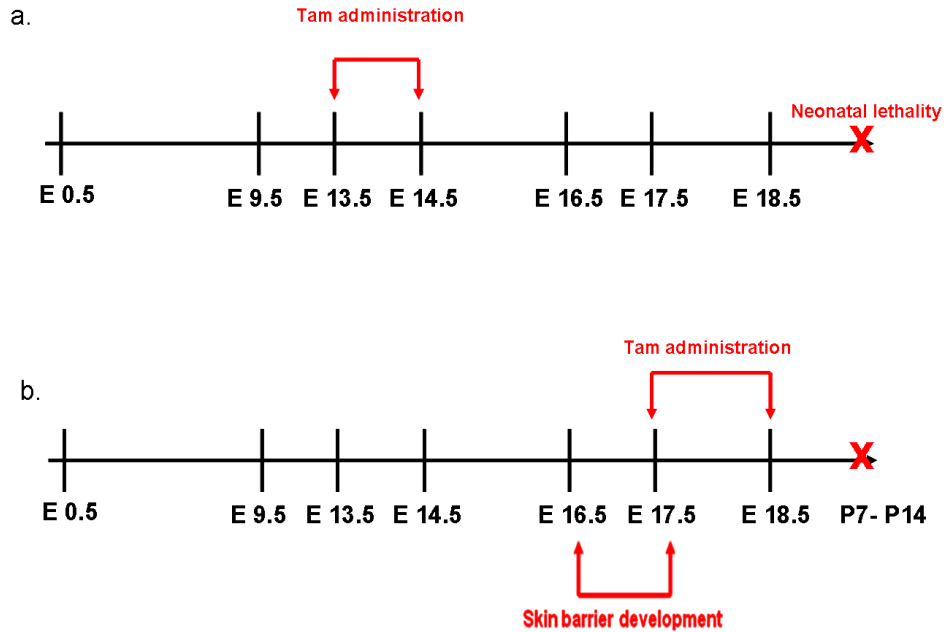
Figure 3. Schematic diagram describes TAM administration. Pregnant females were treated with TAM at different gestational days before (a) and (b) after the start of the EPB development. Intraperitoneal injection of pregnant females at E13.5 and E14.5 (n = 24) leads to neonatal lethality and no pups could be recovered. (b) TAM administration to pregnant females at gestational days 17.5 and 18.5 leads to viable pups. However they died within 7-14 days postnatal (n =12).

To address whether the neonatal lethality is due to an impaired formation of the epidermal barrier, pregnant females from $Pelo^{F/F}CreERT2^{+/-}$ breeding were i.p injected with TAM at gestational stages E13.5 and E14.5, and monitored daily. E18.5 embryos were delivered by caesarean section (Figure 4a). The recovered pups were incubated at 37°C and each individual embryo was monitored for body weight hourly. After incubation, genotyping PCR was performed on the DNA extracting from a small piece of skin. Genotyping analysis revealed the presence of both $Pelo^{F/F}$ and $Pelo^{\Delta/\Delta}$pups (Figure 4b). In agreement with this result, Pelo protein was not detected in skin extracts from $Pelo$-null pups by Western blot analysis (Figure 4c). Thus, $Pelo$ was efficiently ablated in the skin of $Pelo^{\Delta/\Delta}$ pups.

During the incubation time, we observed that $Pelo^{\Delta/\Delta}$ skin was erythematous, glossy and sticky to the touch (Figure 4d). The body weight of $Pelo$-deficient embryos decreased gradually and all E18.5 $Pelo^{\Delta/\Delta}$ embryos died within 5-6 hours of caesarean delivery. In contrast, control $Pelo^{F/F}$ pups did not show significant weight changes during the same period (Figure 4e). These observations suggest that the decrease in body weight of $Pelo^{\Delta/\Delta}$ embryos was due to increased transepidermal water loss resulting from an impairment of their epidermal barrier.

3.1.2 Skin barrier defects are responsible for neonatal lethality in $Pelo^{\Delta/\Delta}$ pups

Epidermal barrier function was investigated using dye penetration assay. Control $Pelo^{F/F}$ and mutant $Pelo^{\Delta/\Delta}$ E18.5 embryos were subjected to toluidine blue dye. In contrast to control embryos, there was extensive skin penetration of toluidine blue dye in $Pelo^{\Delta/\Delta}$ embryos (Figure 4f). These results suggest that the skin barrier defect is responsible for the neonatal lethality in $Pelo^{\Delta/\Delta}$ pups.
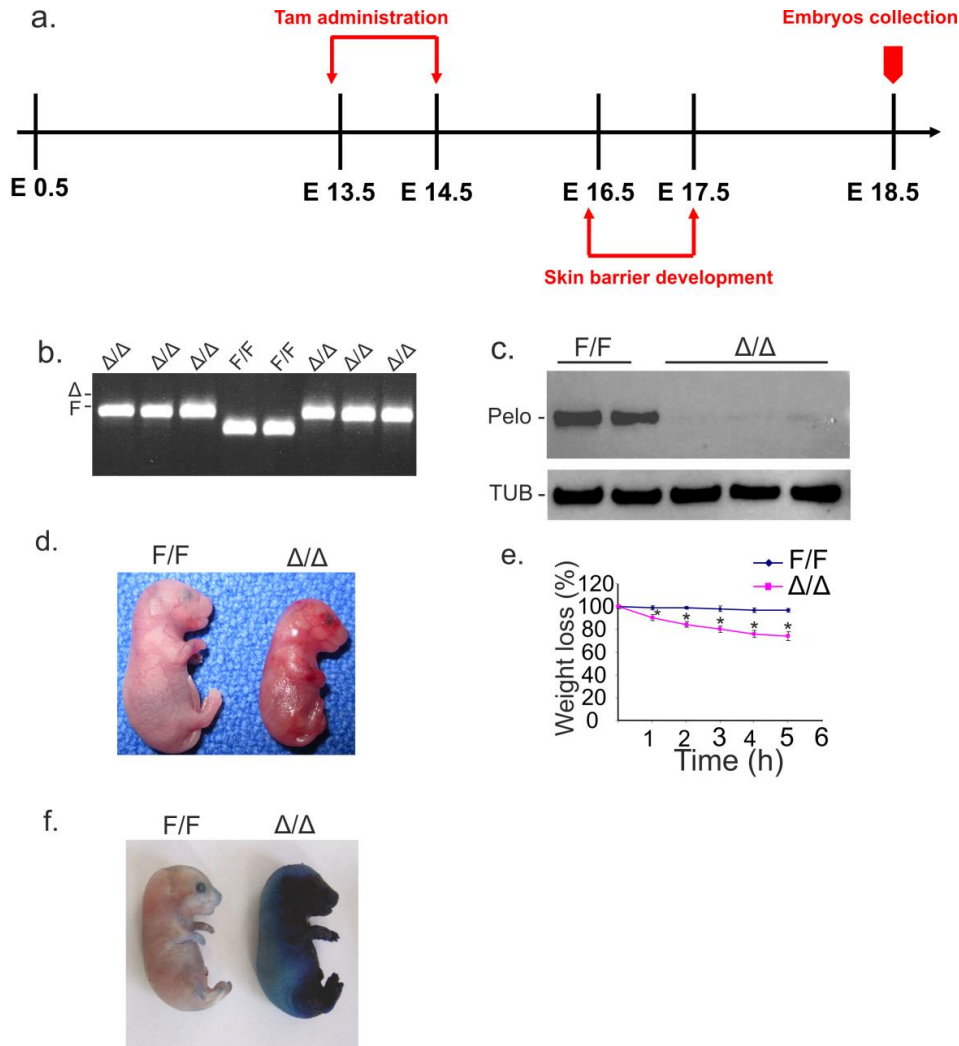
Figure 4.   Temporal deletion of *Pelo* prior to the formation of epidermal barrier leads to perturbation of the epidermal permeability function and early neonatal lethality. (a) Schematic illustration of the TAM administration to the pregnant female mice and the time of embryos collection. (b) Genomic DNA was isolated from the skin of E18.5 embryos and subjected to genotyping PCR analysis. The presence of a 455-bp fragment of *Pelo^Δ* allele (Δ) and loss of a 376-bp of *Pelo^F* allele (F) in mutant skin demonstrates successful Cre-mediated recombination. Note that *Pelo^{F/F}* embryos did not contain the *CreERT* allele (data not shown). (c) Western blot analysis of epidermal lysates from E18.5 *Pelo^{F/F}* and mutant *Pelo^{Δ/Δ}* pups shows efficient loss of Pelo in *Pelo^{Δ/Δ}*, but the presence of Pelo protein in control *Pelo^{F/F}* littermates. For loading control, the blot was stripped and reprobed with anti α-tubulin antibody (TUB). (d) Gross morphology of E18.5 *Pelo^{F/F}* (left) and *Pelo^{Δ/Δ}* (right) pups are shown. (e) Graph showing the weight loss of *Pelo^{F/F}* (n = 4) and *Pelo^{Δ/Δ}* embryos (n = 6) over the indicated time period. Body weight over the time are presented relative to that of 0 h and represented as mean ± SEM. *$P < 0.05$ vs*. control. (f) Skin permeability assay on E18.5 *Pelo^{F/F}* and *Pelo^{Δ/Δ}* embryos using toluidine blue.

To get insight into the underlying cause of EBP defect, histology, differentiation, and proliferation status of the skin of $Pelo^{\Delta/\Delta}$ embryos from E15.5, E 16.5, E17.5 and E18.5 were investigated. Prior to epidermal barrier formation, the histology of *Pelo*-null skin at E15.5 and E16.5 did not reveal any obvious abnormalities compared to control skin. However, after barrier acquisition, the skin of mutant embryos at E17.5 and E18.5 displayed increased epidermal thickening in some regions (Figure 5).
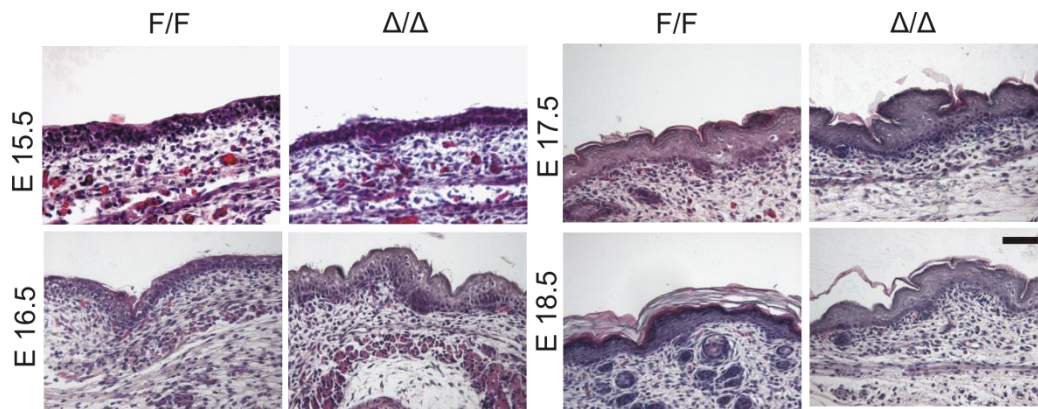
Figure 5. Embryonic development of Epidermis in $Pelo^{F/F}$ and $Pelo^{\Delta/\Delta}$ embryos. Representative images showing the histology of the skin from different embryonic stages E15.5, E16.5, E17.5 and E18.5 of control $Pelo^{F/F}$ and mutant $Pelo^{\Delta/\Delta}$ embryos. Scale bar = 50 µm.

To assess the proliferation status of control and mutant skin, BrdU was intraperitoneally administered to pregnant females and 2 h later skin samples of E18.5 embryos were processed for immunostaining using anti-BrdU and anti-K14 antibodies. *Pelo*-deficient epidermis exhibited a significant elevation in the number of K14-stained basal cells that incorporated BrdU as compared to controls (Figure 6a). Immunohistological analysis did not reveal any differences between control and mutant epidermis in expression of the cell layer-specific marker protein, basal-K14, subrabasal-K10 and granular cell marker loricrin (Figure 6b). Expression of terminal differentiation marker filaggrin (Flg) was first observed in control and mutant granular cell

layers at E17.5 (Figure 6b). At E18.5, Flg accumulated in layers of the stratum granulosum (SG) and in stratum corneum (SC) of control skin. However, in mutant skin, Flg was present in all layers of the SG, but at low levels in the SC (Figure 6b). The low levels of Flg immunostaining in the SC led us to assess whether there were any alterations in the cornified envelop (CE) of mutant embryos. CEs were isolated from the epidermis of the control and mutant embryos as described in the methods. Microscopic analysis showed symmetrical and smooth $Pelo^{F/F}$ CEs. In contrast, $Pelo^{\Delta/\Delta}$ CEs were rough, irregular and aggregated, indicating an immature state of CEs in the mutant epidermis (Figure 6c).

3.1.3 Impaired epidermal barrier acquisition in *Pelo*-deficient pups is associated with altered profilaggrin processing

To investigate whether the altered distribution of filaggrin in the epidermis of E18.5 $Pelo^{\Delta/\Delta}$ pups was due to a defect in filaggrin processing, we performed Wetern blot analysis. As expected, protein blot of epidermal protein lysates revealed that profilaggrin was processed to filaggrin monomers in the epidermis of E18.5 control embryos. In contrast, high levels of profilaggrin derived proteolytic intermediates and almost no filaggrin monomers were detected in *Pelo*-null epidermis. The results from our immunohistochemical and protein analysis suggested that the impaired epidermal barrier acquisition in *Pelo*-deficient pups may be a result of altered profilaggrin processing (Figure 6d). Impaired development of the epidermal barrier in *Pelo*-null embryos prompted us to determine the expression levels of several genes encoding transcription factors and structural proteins that are involved in barrier establishment, including *Kruppel like factor 4* (*Klf4*), *Grainy head–like 3* (*Grhl3*) and *Transglutaminase 1* (*Tgase1*). As shown in Figure 6e, expression levels of *Klf4, Grhl3* and *Tgase1* were significantly higher during and after barrier acquisition in control compared to *Pelo*-deficient epidermis. Collectively, these

results demonstrated that the *Pelo* deletion during embryonic skin formation results in altered

profilaggrin processing, abnormal CE formation and skin barrier defects, which could be the

underlying cause of early neonatal lethality of $Pelo^{\Delta/\Delta}$ pups.
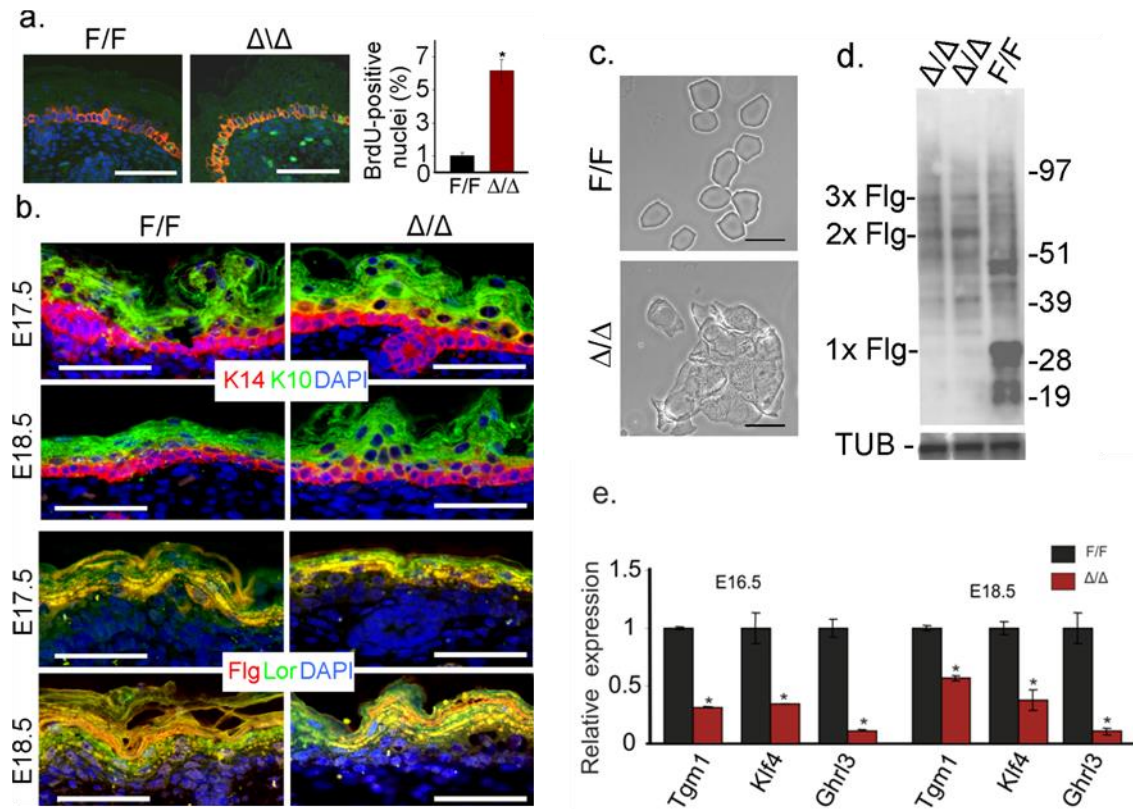
Figure 6. Epidermal skin dysfunction of *Pelo*-deficient mice is a result of aberrant processing of profilaggrin into filaggrin monomers. (a) Epidermal proliferation was assayed in skin sections of E18.5 $Pelo^{F/F}$ and $Pelo^{\Delta/\Delta}$ embryos by co-immunostaining using antibodies to BrdU and k14. All BrdU-positive nuclei were detected in basal cells of $Pelo^{F/F}$ and $Pelo^{\Delta/\Delta}$ epidermis. Scale bar = 40 μm. Histogram showing the percentage of BrdU positive nuclei relative to number of k14 positive cells in the basal layer (right panel). Nuclei (blue) were stained with DAPI. More than 400 cells were examined from 3 pups of each genotype. Values are expressed as mean ± SEM. *$P < 0.05$ *vs.* control. (b) Immunofluorescence of epidermal K10, K14 (left panel) and Loricrin (Lor), filaggrin (Flg) (right panel) in $Pelo^{F/F}$ and $Pelo^{\Delta/\Delta}$ skin sections from E17.5 and E18.5 mice. Scale bar = 100 μm. (c) Morphological appearance of purified cornified envelopes (CEs) from control and mutant E18.5 epidermis visualized by phase-contrast light microscope. Scale bar = 200 μm. (d) Western blot analysis for profilaggrin processing in E18.5 $Pelo^{F/F}$ and $Pelo^{\Delta/\Delta}$ epidermal protein extracts. The positions of profilaggrin-intermediates (2x Flg and 3x Flg) and filaggrin monomers (1x Flg) are indicated on the left, and the positions of molecular weight markers (kDa) are indicated on the right. (e) Quantitative RT-PCR analysis for the expression of epidermal barrier-related genes *Tgm1, Klf4* and *Grhl3* in $Pelo^{F/F}$ and $Pelo^{\Delta/\Delta}$ epidermis from E16.5 and E18.5. Values of expression levels normalized to *Hprt* are presented as mean ± SEM of three independent experiments. Transcript levels of control epidermis were expressed as 1.0. *$P < 0.05$ *vs.* control.

3.1.4 Impaired epidermal barrier formation in *Pelo*-null epidermis is correlated with increased activity of BMP and PI3K/AKT signaling

To determine whether the expression of Pelo in skin is correlated with the epidermal barrier formation, protein blot analysis of epidermal protein lysates from control E15.5, E16.5, E17.5 and E18.5 revealed elevation of Pelo prior to barrier acquisition and significantly down-regulated after barrier formation (Figure 7a). These results were further confirmed by studying the expression pattern of *Pelo* transcripts (Figure 7b). These data indicates that the change in the levels of Pelo during epidermal barrier formation is regulated at the transcription level and reflects the important role of Pelo during the EPB development.

Pervious results showed the role of Pelo in regulating BMP and PI3K/AKT signaling pathways during the differentiation of embryonic and spermatogonial stem cells (Nyamsuren et al. 2014; Raju et al. 2015). This knowledge led us to determine the activity of both signaling pathways during epidermal barrier formation in skin of control and mutant embryos. We investigated the expression levels of phosphorylated isoforms of SMAD 1/5 and AKT, as indicators of the activity of BMP and PI3K/AKT, respectively, in control and mutant epidermis. Like the expression pattern of Pelo, expression levels of pSMAD1/5 were down-regulated after completion of barrier development in control epidermis, but were unchanged in *Pelo*-deficient epidermis (Figure 7c). In agreement with O'Shaughnessy et al. (2009), expression levels of pAKT were elevated at the onset of barrier formation at E16.5 and attenuated thereafter in control epidermis (Figure 7d). In *Pelo*-deficient epidermis, expression of pAKT remained at high levels even after barrier formation (Figure 7d), indicating that Pelo deficiency leads to persistent activation of BMP and PI3K/AKT signaling pathways.
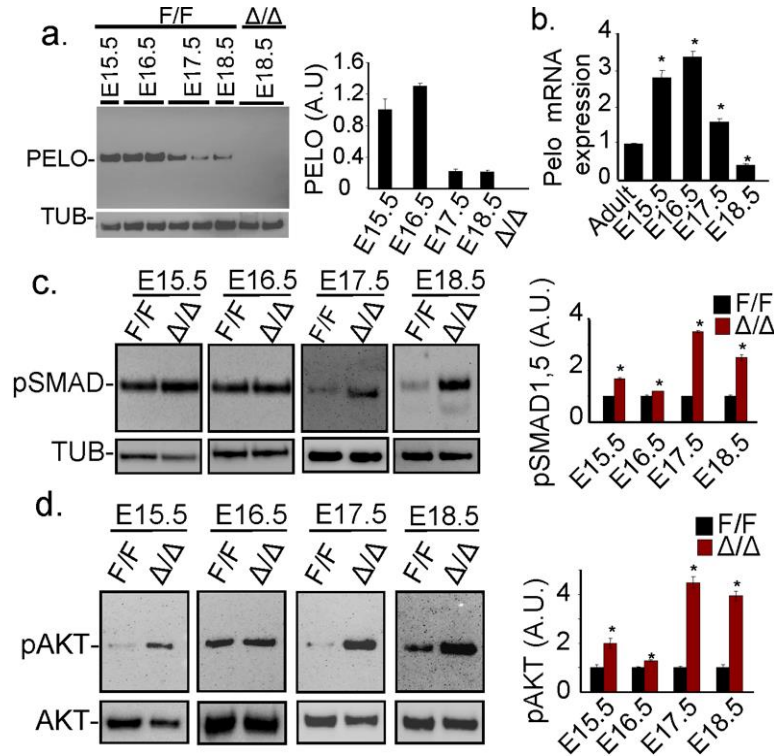
Figure 7. Loss of Pelo elevates the activity of BMP and PI3K/AKT signaling pathways. (a) Protein blot analysis of Pelo expression in epidermal protein extracts of control $Pelo^{F/F}$ embryos during skin barrier acquisition. Epidermal protein extracts from mutant embryos at E18.5 was used to verify the specificity of anti-Pelo antibody. In the right panel, expression levels of Pelo quantified and normalized to that of α-tubulin (TUB) are presented. The Pelo protein levels are presented as mean ± SEM of three experiments. A.U. indicates arbitrary units. Protein levels in epidermis of E15.5 were expressed as 1.0. *P < 0.05 *vs.* E15.5. (b) Epidermal RNA isolated from control embryos at different embryonic stages and adult mice was used to determine the expression levels of *Pelo* by qRT-PCR. Values of *Pelo* expression levels normalized to *Hprt* are presented as mean ± SEM of three experiments. Transcript levels in epidermis of adult mice were expressed as 1.0. *n* = 3 embryos per stage. *P < 0.05 *vs.* adult. (c, d) Western blot analysis showing the expression levels of pAKT (c) and pSMAD1/5 (d) in control $Pelo^{F/F}$ and mutant $Pelo^{\Delta/\Delta}$ epidermis at different embryonic stages (left panels). In the right panels, expression levels of pAKT and pSMAD1/5 normalized to that of total AKT (AKT) and α-tubulin (TUB), respectively, are presented. Expression levels presented as mean ± SEM of three experiments. Protein levels of control $Pelo^{F/F}$ epidermis at each age were expressed as 1.0. *P < 0.05 *vs.* control at the same developmental stage.

To determine whether the impaired formation of skin barrier in *Pelo*-deficient embryo is due to elevated BMP and PI3K/AKT signaling pathways, organotypic cultures with skin explants dissected from E15.5 embryos were performed. Histological analysis of skin explants after two days of culture showed the development of SC in control and mutant (Figure 8a). To determine

the status of the epidermal barrier acquisition in control and mutant skin explants, we examined

the diffusion of the fluorescent dye Lucifer yellow in cultured skin explants. The dye retained in

the upper layer of control explants SC, whereas in mutant explants Lucifer yellow diffused

through the SC down into the dermal layer (Figure 8b). These results supported our *in vivo*

findings and indicate that impaired epidermal barrier acquisition is a result of autonomous

defects in *Pelo*-deficient skin and not due to systemic defects of Pelo deficiency.

To determine whether inhibition of PI3K/AKT signaling can restore epidermal development

in mutant explants, E15.5 skin explants were cultured for 2 days in the presence or absence of

PI3K inhibitor LY294002. Although LY294002 was able to significantly attenuate pAKT levels

in control and mutant explants, these pAKT levels remained significantly higher than the basal

pAKT levels found in control skin explants (Figure 8c). Indeed, histological analysis revealed a

failure of SC development in both control and mutant explants in the presence of PI3K inhibitor

(Figure 8a). Interestingly pSMAD1/5 levels were slightly increased in the LY294002-treated

skin of both genotypes (Figure 8c). These results highlighted that there could be a cross talk

between BMP and PI3K/AKT signaling pathways. Next we addressed whether attenuation of

BMP signaling would impact on PI3K/AKT activity. Skin explants were cultured in the presence

or absence of noggin, a BMP antagonist. The effectiveness of noggin in inhibiting BMP activity

was confirmed by decrease in pSMAD1/5 levels in control and mutant skin explants (Figure 8d).

Upon noggin treatment in mutant explants, we observed a significant decrease in the levels of

pAKT that are corresponded to basal levels observed in control skin (Figure 8d). Importantly, we

observed the development of SC in noggin-treated mutant explants (Figure 8a) and proper

functioning of the skin barrier, as indicated by retention of Lucifer yellow in the upper layer of

SC (Figure 8b). In contrast, inhibition of BMP signaling in control skin explants disrupted the

development of SC (Figure 8a) and affected the EPB, as judged by dye diffusion through all

epidermal layers and into the dermis of noggin-treated control explants (Figure 8b). In support of these results, levels of Flg monomers were markedly attenuated in noggin-treated control skin explants, whereas profilaggrin processing was restored and filaggrin monomers were readily detected in noggin-treated mutant skin explants (Figure 8e).

Taken together these results support our conclusion that the restoration of epidermal barrier function by noggin treatment in *Pelo*-deficient pups is accompanied by proper processing of profilaggrin. These results also establish a direct link between elevated levels of BMP and PI3K/AKT signaling with defective filaggrin processing in *Pelo*-deficient epidermis.
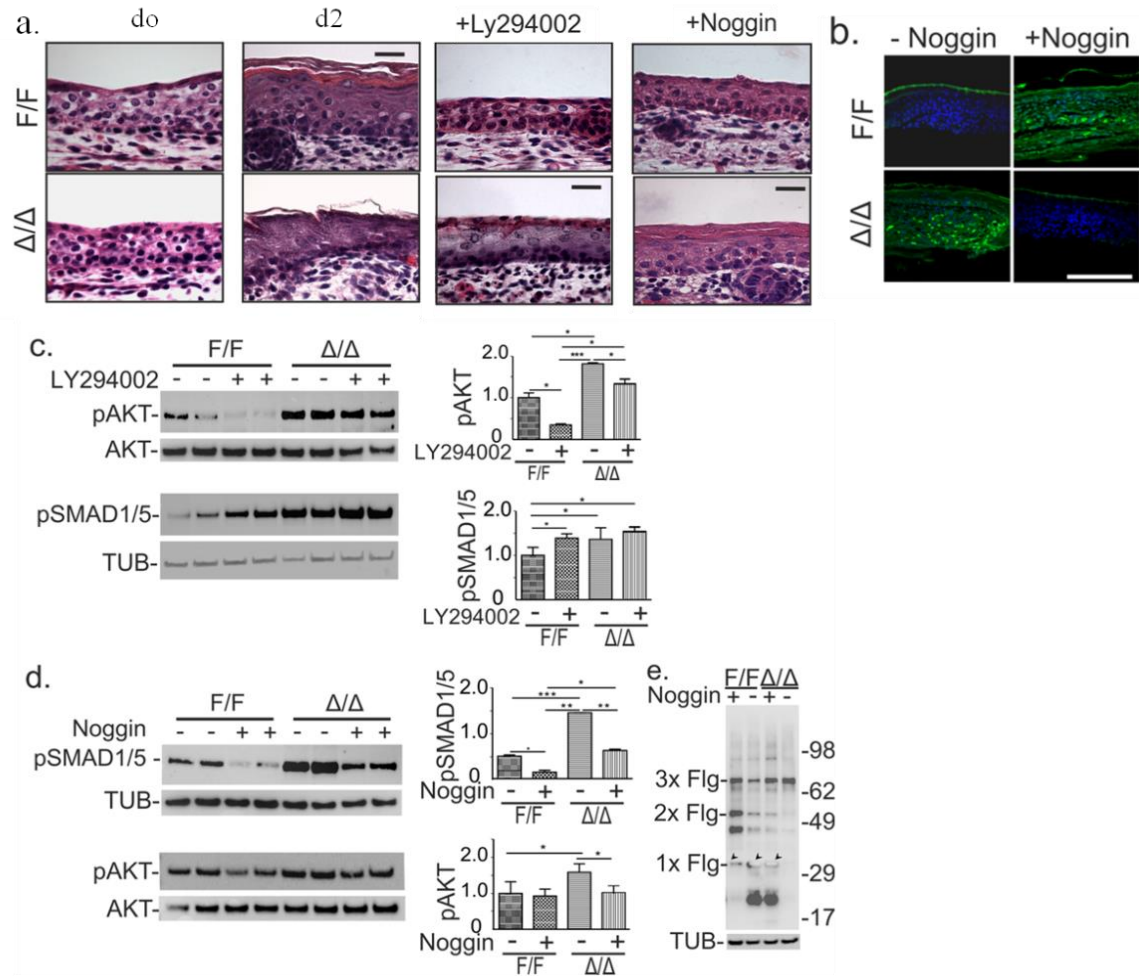
Figure 8. Noggin treatment restores the functional EPB in mutant skin organotypic culture. (a) Histological analysis of E15.5 *Pelo^{F/F}* and *Pelo^{Δ/Δ}* skin explants before (d0) and after culture for 2 days (d2), and cultured skin explants in the presence of LY294002 or Noggin. (b) Micrographic images showing Lucifer Yellow dye applied on *Pelo^{F/F}* and *Pelo^{Δ/Δ}* skin explants cultured in presence (+) or absence (-) of Noggin. Scale bars in a= 20 μm and in b=40 μm. (c, d) Western blot showing pAKT and pSMAD1/5 protein levels in protein extracts derived from *Pelo^{F/F}* and *Pelo^{Δ/Δ}* skin explants cultured either with (+) or without (-) PI3K inhibitors LY294002 (c) or recombinant Noggin (d). Histograms in right panels show the expression levels of pAKT and pSmad1/5 normalized to that of total AKT (AKT) and α-tubulin (TUB), respectively. Expression levels are presented as mean ± SEM of three experiments. Protein levels in untreated skin explants from control embryos were expressed as 1.0 A. U. indicates arbitrary units. *$P < 0.05$, **$P < 0.001$, ***$P < 0.0001$ *vs.* untreated control or mutant. (e) Protein blot analysis for profilaggrin processing in protein extracts of skin explants cultured in either presence (+) or absence of Noggin (-). The positions of profilaggrin-related protein products are indicated on the left, and the positions of molecular weight marker (kDa) on the right.

3.1.5 Deletion of *Pelo* after skin barrier formation results in postnatal hyperproliferative skin disorder

To further analyze the phenotypic changes in the skin of $Pelo^{\Delta/\Delta}$ mice after birth, TAM was twice administered to pregnant females on gestational days 17.5 and 18.5 (after the development of the skin barrier) to avoid early neonatal lethality (Figure 9a). Obvious defects in the epidermal barrier were observed in $Pelo^{\Delta/\Delta}$ pups during the first days after birth in the form of severe dehydration, scaliness, hair loss, and they died subsequently between postnatal P7- P14 days. Histological analyses of skin sections from $Pelo^{\Delta/\Delta}$ pups displayed epidermal hyperplasia as well as hyperkeratosis and dermal inflammatory cell infiltrate (Figure 9b). Immunohistochemical analyses showed increased thickness in all epidermal layers (Figure 9c).
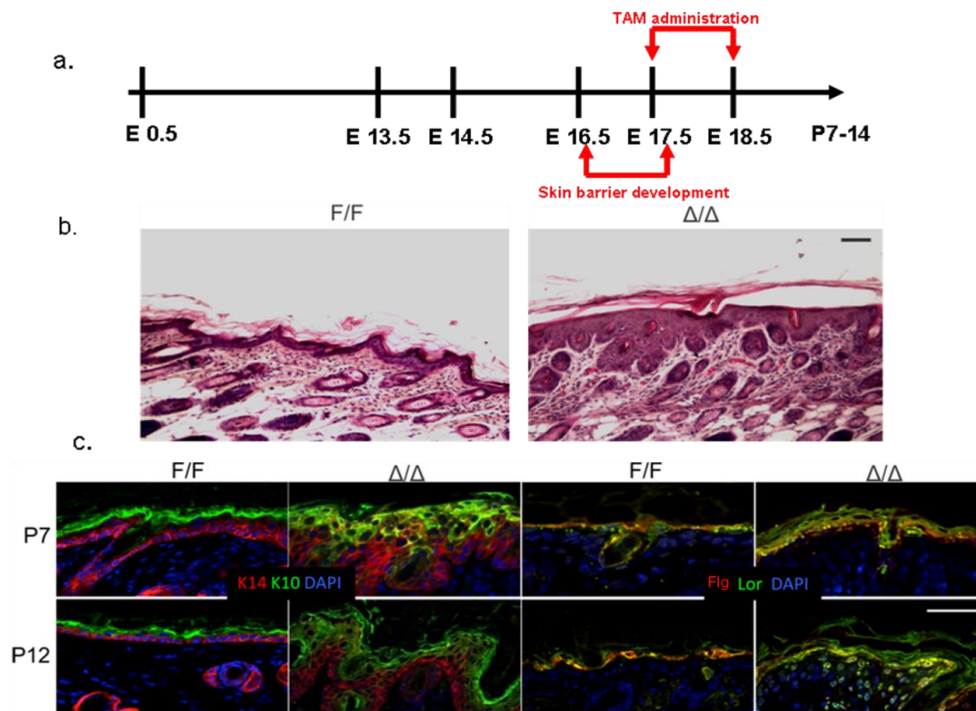
Figure 9. Analysis of skin sections from $Pelo^{F/F}$ and $Pelo^{\Delta/\Delta}$ pups. (a) Schematic diagram describes Tamoxifene administration to $Pelo^{F/F}$ pregnant mice at gestational days E17.5 and E 18.5 resulted in viable pups for 7 to 14 days. (b) Hematoxylin/eosin-stained skin sections from the neck region of control (F/F) and mutant mice (Δ/Δ). Histological analysis of mutant skin showed epidermal thickening, hyperkeratosis and inflammatory dermal infiltrate. Scale bars =100 μm (c) Immunohistochemistry with different epidermal markers, anti-K14, anti-K10, anti- loricrin and anti-filaggrin, Sections were counterstained with DAPI. Scale bars 100 μm.

3.1.6 Epidermal barrier defect in *Pelo*-deficient mice leads to hyperkeratosis and inflammation

To investigate whether impaired barrier function results in increased susceptibility to skin inflammation in adult $Pelo^{\Delta/\Delta}$ mice as showed in other mouse models with a defect in skin barrier acquisition (Boguniewicz and Leung 2011), we injected 8-week-old $Pelo^{F/F}$, $Pelo^{F/+}CreERT2$ and $Pelo^{F/F}CreERT2$ mice with TAM for 5 subsequent days. By 2-4 months after TAM administration, control $Pelo^{F/F}$ and $Pelo^{\Delta/+}$ mice presented a normal skin appearance (Figure 10a), whereas the tails and ears skin of $Pelo^{\Delta/\Delta}$ mice were scaly. In addition, facial and neck areas exhibited alopecia, erythema and ulcerations, which were aggravated by increased scratching behavior that worsened with time (Figure 10b). Therefore, *Pelo*-deficient animals had to be sacrificed once these symptoms appeared to minimize suffering. Histological analysis revealed marked epidermal hyperplasia, and a compact and hyperkeratotic stratum corneum in the skin of $Pelo^{\Delta/\Delta}$ mice (Figure 10c and d). The hair follicles were hyperplastic, consistent with the alopecic phenotype in $Pelo^{\Delta/\Delta}$ mice (Figure 10d). Electron microscopic analysis revealed an enlarged corneal epidermal layer with thick, non-condensed and loosely connected corneal sheaths of different electron density exclusively in skin sections of adult $Pelo^{\Delta/\Delta}$ (Figure 11). In addition, a massive diffuse inflammatory infiltrate was observed in the dermis of $Pelo^{\Delta/\Delta}$ mice as detected by a significant increase in the number of mast cells in skin sections stained with Toluidine blue (Figure 10e-g).
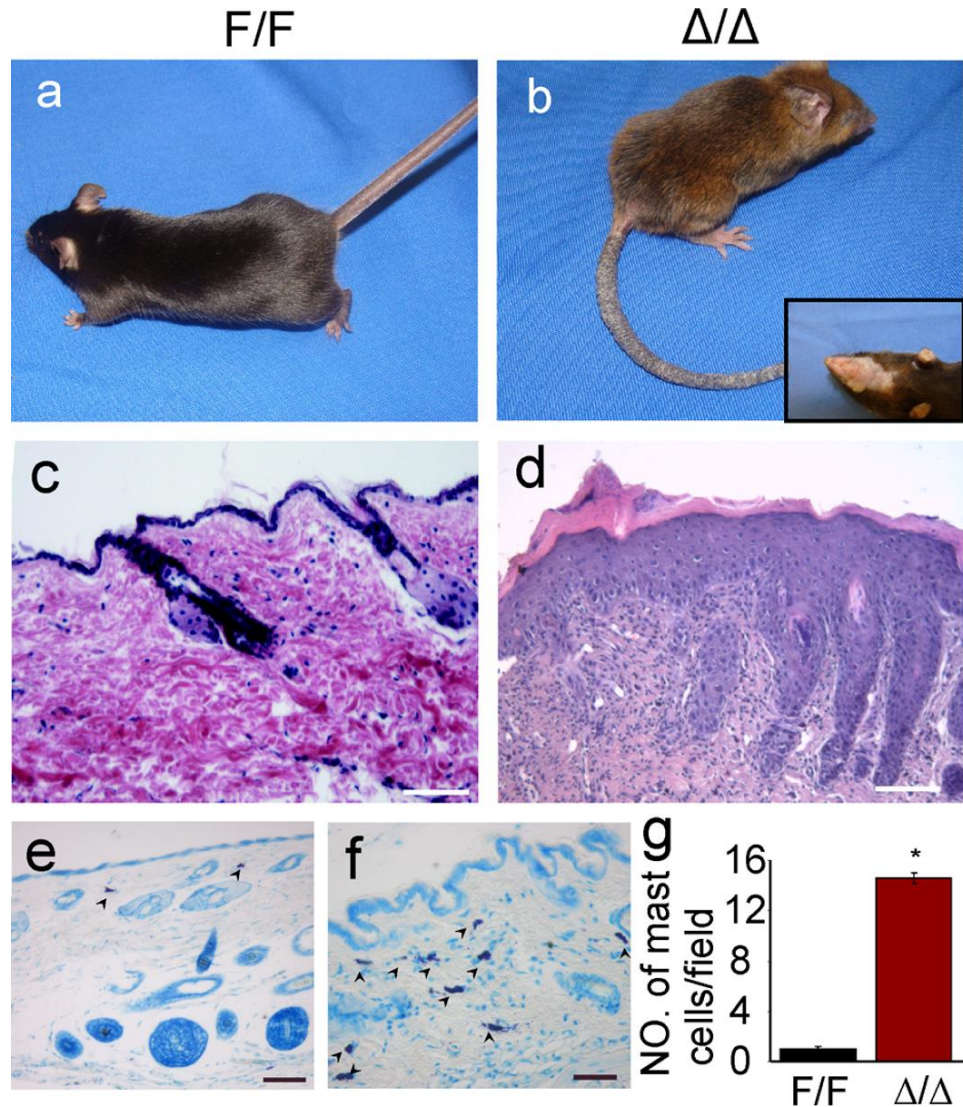
Figure 10. Depletion of Pelo during mouse adult life displays atopic dermatitis-like phenotypes. (a, b) Gross morphology of control (a) and mutant (b) mouse after 3 months of TAM administration. Alopecia is noticed in the neck region of mutant mice (insert in b). (c, d) Hematoxylin/Eosin-stained skin sections from the neck region of control (c) and mutant mice (d) Scale bars (c,d) = 100 μm. (e, f) Toluidine blue-stained sections of *Pelo*^{F/F} (e) and *Pelo*^{Δ/Δ} (f) skin. Arrowheads indicate mast cells with intense blue colour in the dermis. Scale bars (e,f) = 50 μm (g) Number of mast cells in skin sections of *Pelo*^{F/F} and *Pelo*^{Δ/Δ} animals is represented as mean ± SEM. *$P > 0.05$. Data represent the number of mast cells in 20 microscopic fields from 3 animals per genotype.
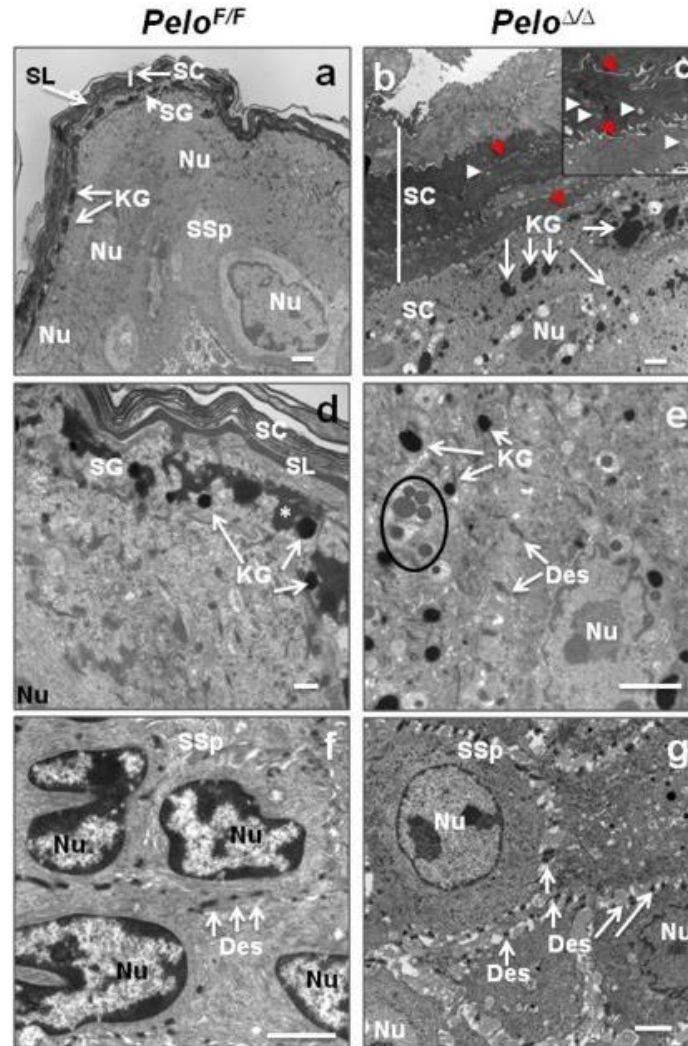
Figure 11. Representative TEM images of skin sections from the neck region of control *Pelo^{F/F}* and mutant *Pelo^{Δ/Δ}* mice. Epidermis of *Pelo^{Δ/Δ}* mice presents with thickened over-compacted stratum corneum (SC) layers with different electron density and microvesicular inclusions (white arrowheads; **b, c**). *Pelo*-null mice displayed an extended layer of stratum granulosum (SG) layer with nucleated (Nu) cells containing many keratohyalin granules (KG) of different sizes (**b, e**) and containing less electron dense material considered immature KG (circled) (**e**). Desmosomes were detected in the stratum spinosum in all mice (**f, g**). Control skin displayed a distinct small layer of SG with electron dense deposits of keratin (*) and KG (**a, d**). In all TEM images, the epidermal surface is always located at the top of the image. Bars = 100 nm (a, b), 500 nm; 2 μm (d-g).

To assess whether the inflammatory skin phenotype is a result of impaired keratinocyte differentiation, we determined the expression profile of specific markers of different epidermal layers. As shown in Figure 12a and b, K14 was expressed in basal cells of control epidermis, whereas it extended into the supra-basal cell layers of mutant epidermis and overlapped with

expression of the early differentiation marker K10 (Figure 12c and d). Expression of late differentiation markers, loricrin and filaggrin, revealed increased layers of SG and SC in mutant epidermis (Figure 12e-h) indicating perturbed keratinocyte differentiation is the cause for disruption of epidermal barrier function in adult mutants.

Next, we addressed the origin of the inflammatory phenotype and investigated whether it correlated with epidermal hyperplasia and scratching behavior in $Pelo^{\Delta/\Delta}$ mice. Expression levels for epidermal IL-4 and TSLP, which are implicated in the pathogenesis of atopic dermatitis (Chan et al. 2001; Demehri et al. 2009), were dramatically increased in $Pelo^{\Delta/\Delta}$ epidermis compared to those of $Pelo^{F/F}$ mice (Figure 12i and j). In addition, mutant mice also showed increased serum IgE levels when compared to control mice (Figure 12k).
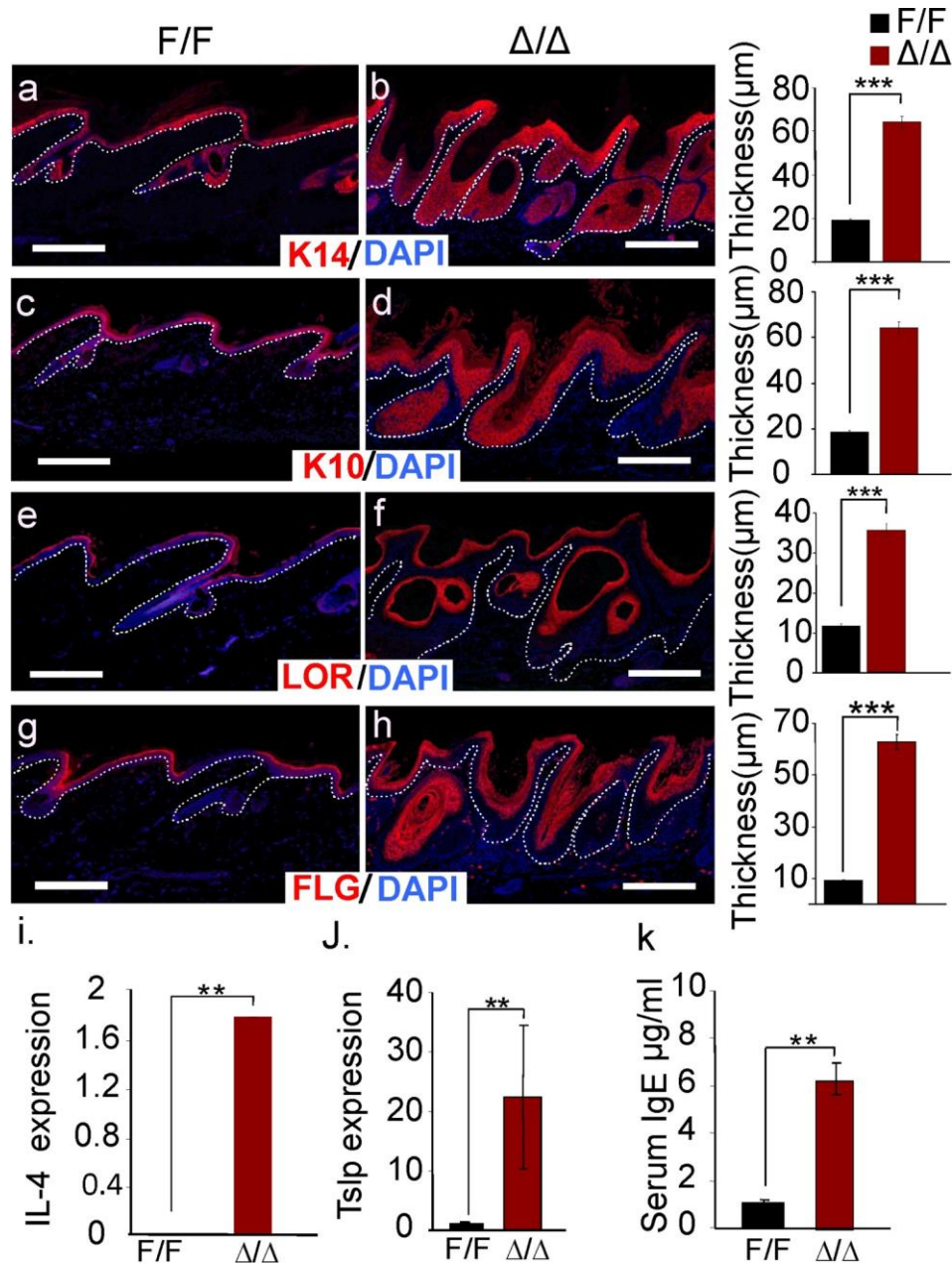
Figure 12. Immunohistochemical analysis for keratinocytes differentiation in *Pelo^F/F*and *Pelo^Δ/Δ*animals. Skin sections derived from the neck region of *Pelo ^F/F*and *Pelo^Δ/Δ* mice were immunostained with anti-K14 (A, B), anti-K10 (C, D), anti- loricrin (E, F) and anti-filaggrin (G, H). Sections were counterstained with DAPI. Dotted line indicates the epidermal dermal boundary. Scale bar = 100 μm. Histograms show thickness of stained layers (right panels). Error bars denote mean ± SEM. ***$P < 0.0001$ *vs.* control. (I, J) Relative expression levels of IL4 and TSLP in epidermis of *Pelo ^F/F*and *Pelo ^Δ/Δ* were determined by qRT-PCR analysis. All values are represented as mean ± SEM. **$P < 0.001$ *vs.* control, $n = 3$-4 animals per genotype. (K) IgE levels were determined in serum of *Pelo ^F/F*and *Pelo^Δ/Δ* mice using ELISA. All values are represented as mean ± SEM. **$P < 0.001$ *vs.* control, $n = 3$-4 animals per genotype.

To determine whether the skin symptoms were due to a systemic immune disorder or a defective skin barrier, we topically administrated TAM daily for 10 days to a small part of $Pelo^{F/F}$ $CreERT2$ tail skin. As vehicle control, tail skin of $Pelo^{F/F}$ $CreERT2$ was treated with ethanol. Six weeks after topical application of TAM, no obvious alternations were observed in vehicle-treated tail skin (Figure 13a), whereas TAM -treated tail skin became thickened and scaly. No other sites of the tail or body skin extending beyond the sites of TAM application exhibited any skin abnormalities (Figure 13b). Histological analyses revealed hyperplasia in these skin lesions (Figure 13c and d).
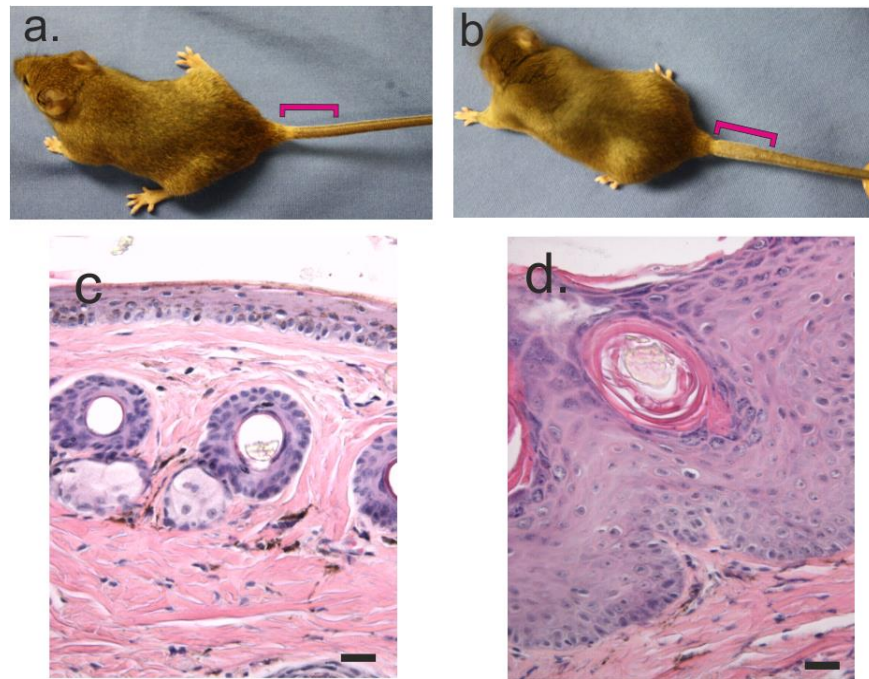
Figure 13. Topical deletion of *Pelo* leads to skin defect. Images showing tail skin of $Pelo^{F/F}CreERT2$ mice were treated by topical application of ethanol as vehicle control (a) or TAM (b). Bracket denotes the treated region. The TAM-treated tail region shows thickening and is scaly. (c,d) H&E stained tail skin sections of ethanol- (c) and TAM-treated (d) tail regions. Scale bar = 20 μm.

3.2 Elucidating the consequence of *Pelo* deletion on embryonic stem cells (ESCs) differentiation

In this study, we attempted to identify the molecular cause for impaired differentiation of the *Pelo*-deficient ESCs. We wanted to address whether Pelo modulates PI3K/AKT signaling pathway as well as other related signal cascades e.g Wnt/ß-catenin, which are known to be important in regulating ESC self-renewal and differentiation (Lee et al. 2009).

3.2.1 Pelo negatively regulates the PI3K/AKT signaling in ESCs

Phosphorylation levels of AKT (pAKT) serves as an indirect quantification of the activity of PI3K/AKT signaling. To check whether Pelo regulates PI3K/AKT signaling pathway in ESCs, we examined the expression of pAKT by Western blot analysis. To avoid the effect of growth factors presenting in serum, ESCs were cultured on mouse embryonic fibroblasts (MEF) in knock out serum replacement medium (KSR) in absence of leukemia inhibitory factor (LIF), as LIF can activate PI3K-AKT pathways (Takahashi et al. 2005). After 24 hours of culture, protein extracts were isolated and subjected to protein blot analysis. As shown in Figure 14a, levels of phosphorylated AKT protein (pAKT) were significantly increased in extracts of $Pelo^{\Delta/-}$ ESCs compared to that of control. These results are consistent with our pervious finding that the activity of PI3K/AKT in testis is negatively regulated by Pelo (Raju et al. 2015).

Several growth factors including basic fibroblast growth factor (bFGF) and epidermal growth factor (EGF) activate the PI3K/AKT signaling (Nii et al. 2014; Wang et al. 2000). To determine whether the bFGF and EGF induce the activity of the PI3K/AKT signaling pathway, $Pelo^{F/-}$ and $Pelo^{\Delta/-}$ ESCs were cultured overnight in KSR medium lacking LIF and treated with either bFGF (20 ng/ml) or EGF (30ng/ml) for 15 min. Immunoblot analysis revealed that the levels of basal pAKT were significantly higher in mutant ESC compared with control, and that both bFGF and

EGF treatment further enhanced the activity of AKT signaling in mutant and control ESCs (Figure 14b).   To study the effect of Wortaminin, a specific inhibitor of PI3K, on the levels of pAKT, *Pelo^{F/-}* and *Pelo^{Δ/-}* ESCs were cultured overnight in KSR medium either in presence or absence of Wortaminin. As shown in Figure14c, levels of pAKT were significantly decreased after the treatment of mutant and control ESCs with Wortaminin. These results indicate that enhanced levels of pAKT are induced in PI3K-dependent manner. Taken together, these data indicate that Pelo negatively regulates the PI3K/AKT signaling in ESCs.
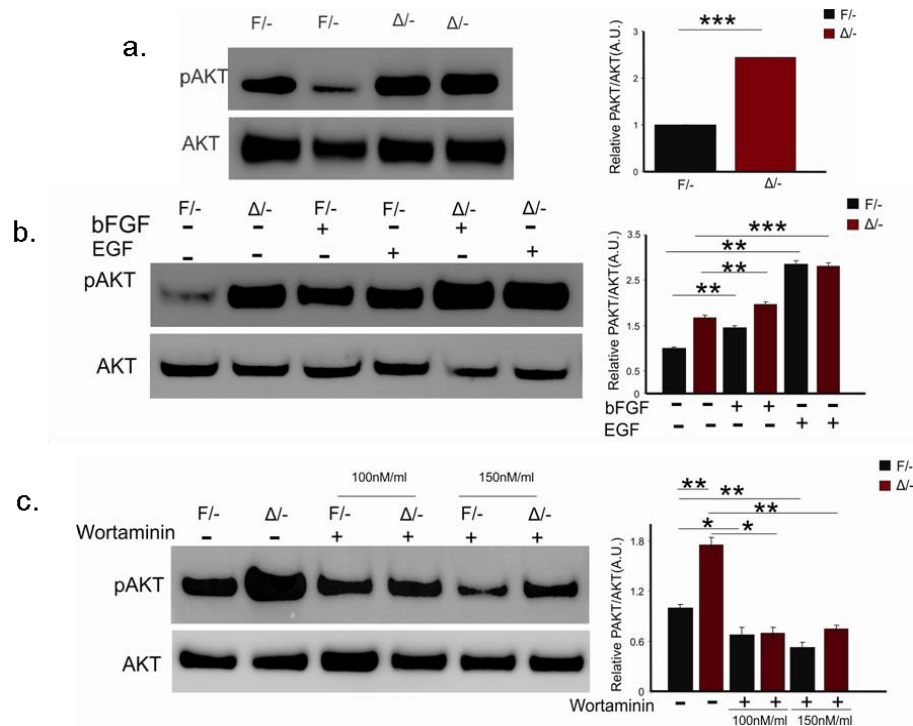
Figure 14. PI3-Kinase/AKT activity in *Pelo^{F/-}*and *Pelo^{Δ/-}* ESCs. Expression levels of pAKT normalized to that of total AKT (AKT) in *Pelo^{F/-}*and *Pelo^{Δ/-}* ESCs (a) and (b) in presence (+) or absence (-) of either bFGF or EGF. (c) Expression levels of pAKT in mutant and control of ESCs in absence (-) or presence (+)PI3K inhibitor (Wortaminin) at 100−150 nM/ml. Histograms in the right panels show the expression levels of pAKT normalized to that of total AKT (AKT). Expression levels are presented as mean ± SEM of three experiments. Protein levels in control (a) and untreated control ESCs (b, c) were expressed as 1.0. A. U. indicates arbitrary units. *$P < 0.05$, **$P < 0.001$, ***$P < 0.0001$ *vs.*untreated control or mutant.

3.2.2 Elevated activity of PI3K/AKT is not the cause for impaired differentiation of *Pelo*-deficient ESCs

To elucidate whether increased activity of PI3K/AKT signaling in mutant $Pelo^{\Delta/-}$ ESCs is responsible for impaired differentiation capacities of $Pelo^{\Delta/-}$ ESCs, $Pelo^{F/-}$ and $Pelo^{\Delta/-}$ ESCs were seeded at a low density and cultured for 12 days in the absence of LIF. The differentiation status was examined at different time points by cell morphology, and the expression of alkaline phosphatase (ALP) and Oct4, specific markers of undifferentiated ES cells. After 12 days of culture, peripheral cells of majority $Pelo^{F/-}$ colonies exhibit flatten morphology and did not express ALP. In contrast, mutant ESCs retained a low cytoplasm-to-nuclei ratio and formed round and multi-layered colonies, which are characteristics of undifferentiated ESCs, and expressed high ALP activity even after 12 days of culture under differentiation condition (Figure 15a). Expression levels of Oct4 were maintained at high levels in mutant ESCs during 12 day culture, while that in control cells was significantly attenuated. These results suggest the impaired potential of mutant ESCs for differentiation (Figure 15b).

Recently, it has been reported that inhibition of PI3K/Akt induces differentiation of mouse and human ESCs (Paling et al. 2004). We plated $Pelo^{F/-}$ and $Pelo^{\Delta/-}$ ECSs at a low density and cultured for 12 days in the absence of LIF and further cultured with and without PI3K inhibitor, Wortaminin. $Pelo^{F/-}$ ESCs showed the differentiated phenotype and reduction in Oct4 expression. Surprisingly $Pelo^{\Delta/-}$ maintained self-renewal even after addition of Wortaminin and showed elevated Oct4 expression levels (Figure 16a, b). These results suggest that the elevated levels of PI3K/AKT signaling are not responsible for the impaired differentiation of mutant ESCs.
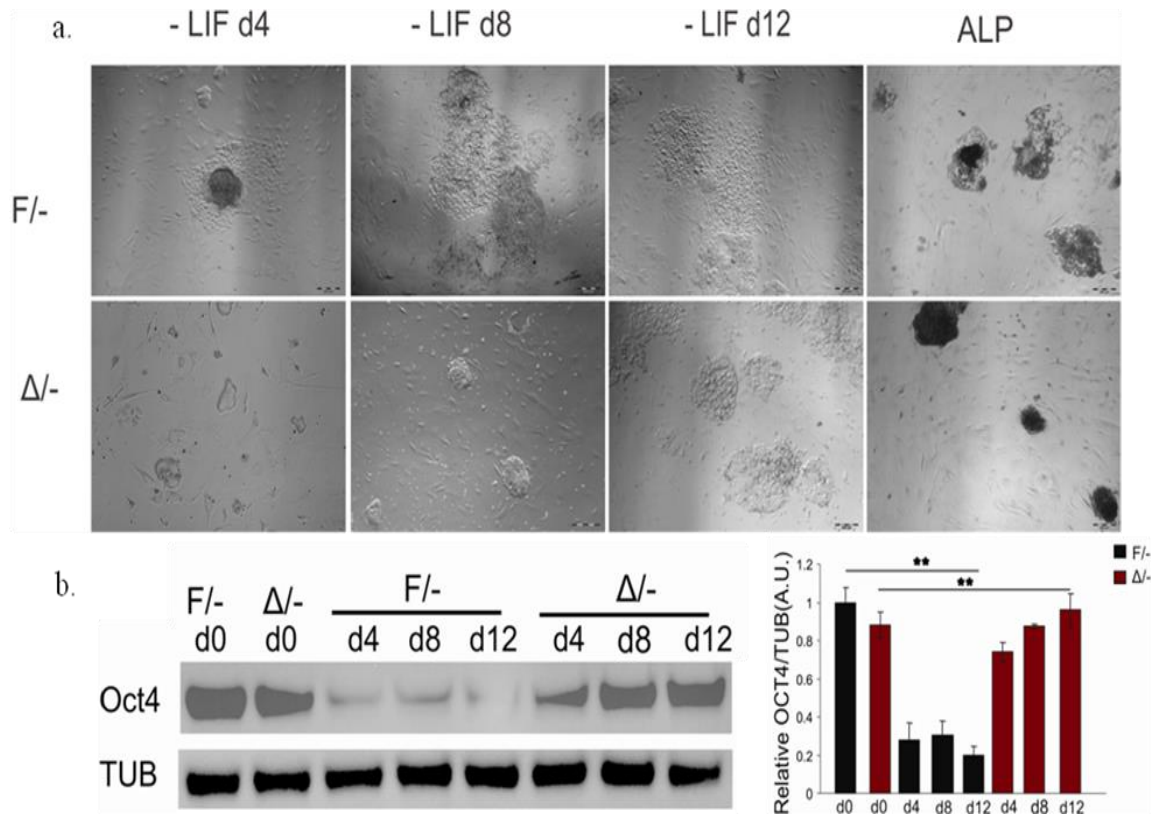
Figure 15. LIF-independent maintenance of pluripotency in *Pelo*^Δ/- ESCs. (a) Morphology of ESCs colonies at day 4, day8 and day12 of culture in absence of LIF. *Pelo*^Δ/- ESCs colonies exhibit the morphology of undifferentiated cells and expressed high levels of pluripotency-related enzyme ALP. Scale Bar = 200µm. (b) Immunoblot for expression of OCT4 in control (F/-) and mutant (Δ/-) ESCs before (d0) and at different times of culture under differentiation condition. In the Bar graph presented in the right panel, expression levels of OCT4 were normalized to that of tubulin (TUB). Values are presented as mean ± SEM. **$P < 0.001$ compared with control.
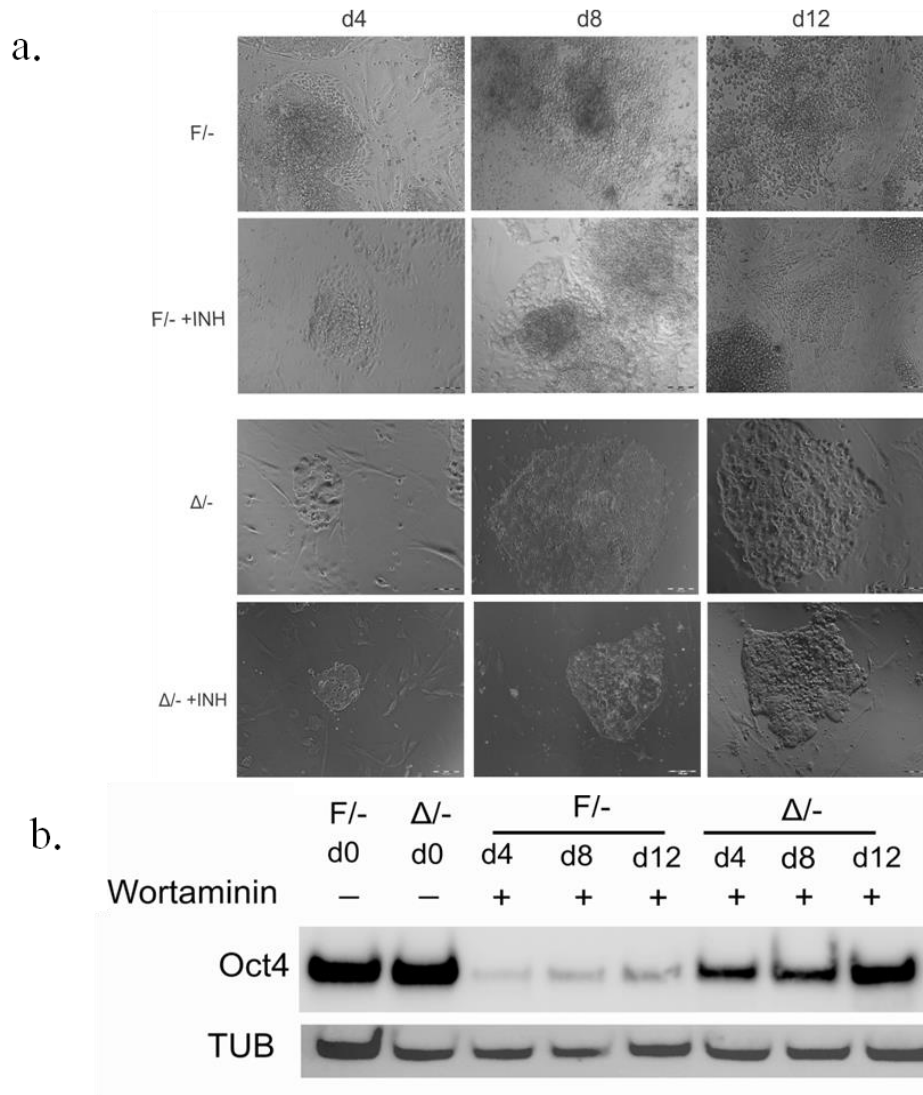
Figure 16. Wortaminin did not induce differentiation in *Pelo*^{Δ/-} ESCs. (a) Morphology of ESCs colonies at day 4, day8 and day12 of culture in absence of LIF, with (+) and without (-) Wortaminin. *Pelo*^{F/-} ESCs differentiate spontaneously in absence of LIF as well as in absence of LIF with Wortaminin. *Pelo*^{Δ/-} retained the characteristic features of undifferentiated ES cells even after Wortaminin treatment. Scale Bar = 100µm. (b) Immunoblot showed expression of OCT4 in control (F/-) and mutant (Δ/-) ESCs before (d0) and at different times of culture under differentiation conditions in presence of Wortaminin. The same immunoblot was stripped and reprobed with the anti-tubulin (TUB) to show equivalence of loading.

3.2.3 Retinoic acid (RA) induces the differentiation of *Pelo*-deficient ESCs

RA, the most potent metabolite of retinol, is an important player for the induction of ESC differentiation (Gudas 1994). To examine the ability of retinoid signaling to promote the differentiation of *Pelo*-deficient ESCs, all-trans RA (atRA) was added after 12 hours of ESC culture in KSR medium lacking LIF. Both $Pelo^{F/-}$ and $Pelo^{\Delta/-}$ ESCs were differentiated as judged by flatted morphology and induction of Dab2 expression, a specific marker for ExEn (Figure 17a, b).These results indicates that the impaired differentiation of *Pelo*-null ESC can be restored by RA. Based on the fact that the retinol retains the ESC pluripotency and its final product RA induces differentiation, we suppose that the retinol metabolism is affected in *Pelo* mutant ESCs. To prove our suggestion, we checked the expression levels of (stimulated by RA gene 8) *Stra8* (Oulad-Abdelghani et al. 1996). Expression levels of *Stra8* were significantly high during differentiation in control ESCs. In contrast, *Stra8* expression levels in $Pelo^{\Delta/-}$ ESCs were low on the basal level d0 and even become lower during differentiation (Figure 17c). Collectively, these results indicate defect in the retinol metabolism in *Pelo*-null ESCs, judged by low *Stra8* levels, leading to defect in ESCs differentiation.

3.2.4 Crosstalk of Foxo1 with β-catenin may be the cause for sustained expression of pluripotent-related genes and impaired differentiation of mutant ESCs

FOXO proteins are negatively regulated by AKT (Brunet et al. 1999). It was reported that Foxo1 regulates *Rdh* expression, which catalyze the retinol metabolism (Obrochta et al. 2015). To address whether Foxo1 function is affected in $Pelo^{\Delta/-}$ ESCs, ESCs were cultured under differentiation conditions for 12 days, and nuclear lysate of $Pelo^{F/-}$ and $Pelo^{\Delta/-}$ ESCs were isolated at different time points and subjected to immunoblotting using anti-Foxo1 antibody (Figure 18a).
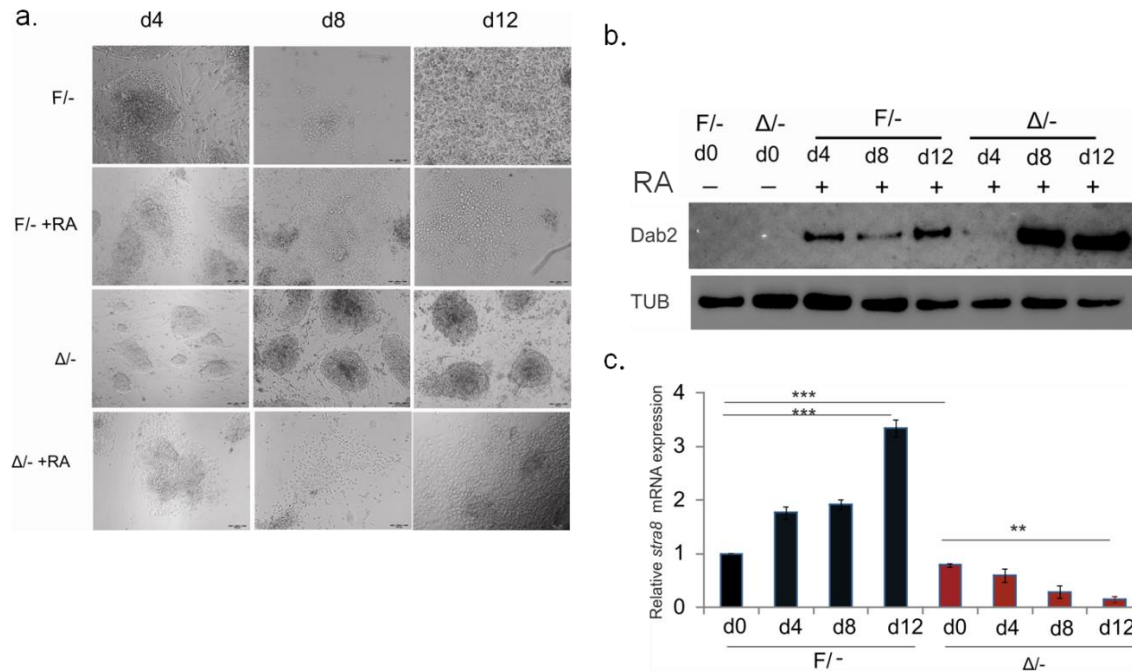
Figure 17. Retinoic acid induces differentiation of *Pelo*^Δ/- ESCs (a) ESCs morphology at d4, d8 and d12 of culture in absence of LIF and with (+) or without (-) of atRA (1 µM/L). RA induces differentiation of control and mutant ESCs. Bar = 100µm. (b) Immunoblot for expression of Dab2 in *Pelo*^F/− and *Pelo*^Δ/- ESCs at different times of culture in presence of RA. (c) Quantitative RT-PCR analysis for the expression of *stra8* in *Pelo*^F/- ESCs and *Pelo*^Δ/- ESCs at different times of culture in absence of LIF. Values were normalized to *Hprt* and are presented as mean ± SEM of three independent experiments. Transcript levels of control ESCs d0 were expressed as 1.0. **$P < 0.001$, ***$P < 0.0001$ *vs.* control.

Nuclear accumulation of Foxo1 in *Pelo*^F/− ESCs at d4 of differentiation was significantly lower than that in mutant cells and depleted thereafter. In contrast *Pelo*^Δ/- ESCs showed persistent Foxo1 nuclear localization after different time points of culture under differentiation condition (Figure 18a). These results interfere with our expectation that activation of PI3K/AKT in mutant ESCs induce phosphorylation and nuclear exclusion of Foxo1. However, our results were in agreement with Zhang et al. (2011) finding, which showed the nuclear localization and transcriptional activation of Foxo1 despite its phosphorylation by AKT pathway. Recent studies identified Foxo1 as a novel interacting partner of β-catenin (Essers et al. 2005). The direct interaction between β-catenin and FOXO1 leads to their nuclear accumulation and enhances

FOXO transcriptional activity. On the other hand, FOXO competes with TCF for interaction with the β-catenin, thereby inhibiting TCF transcriptional activity (Iyer et al. 2013). To check whether nuclear accumulation of Foxo1 in *Pelo*-deficient ESCs results in inhibition of TCF transcriptional activity, control and mutant ESCs were transiently transfected with luciferase-based β-catenin/TCF (TOP/FOP-FLASH) reporters. In the TOP- and FOP-FLASH reporter, the luciferase gene (Luc) under the control of promoter contains multiple copies of optimal and mutant TCF binding sites, respectively. The relative TOP-Luc activities were significantly lower in *Pelo*-deficient ESCs than that in control cells (Figure 18b), indicating the inhibition of TCF transcriptional activity in mutant cells. These results suggest that nuclear accumulation of Foxo1 in *Pelo*-deficient ESCs may be responsible for the sustained expression of pluripotent-related genes even during culture in differentiating conditions. Furthermore, decreased TCF transcriptional activity in mutant cells may explain the observed decrease in proliferation capacity of mutant ESCs. This finding has to be confirmed by analysis the expression of cyclin-D1, a marker of cell division and a target of TCF gene activation (Shtutman et al. 1999).
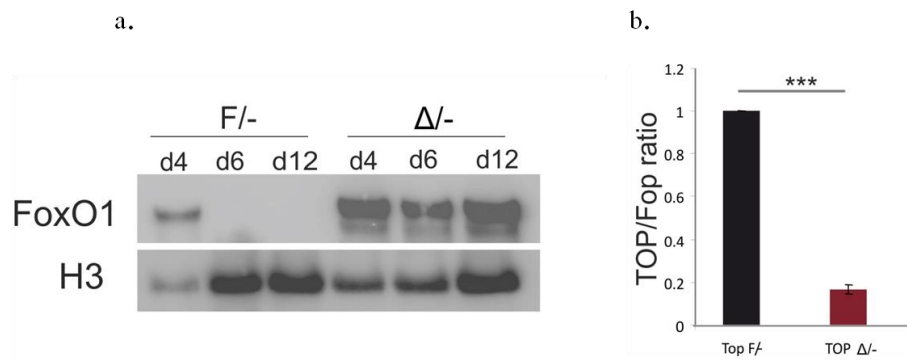
Figure 18. Nuclear localization of Foxo1 in *Pelo*$^{\Delta/-}$ ESCs is associated with low β-catenin/TCF transcription activity. (a) Immunoblot for expression of of nuclear lysate of FoxO1 in *Pelo*$^{F/-}$ and *Pelo*$^{\Delta/-}$ ESCs at different times of culture under differentiation condition. Anti-Histone 3(H3) was used as a loading control. (b) Cells were transfected with pTOP glow or pFOP glow, together with Renilla as an internal control; luciferase activity was measured after 36 h. The ratio of TOP over FOP is plotted. Data presented are mean ± SEM. ***$P < 0.001$ compared with control of three independent experiments.

4. Discussion

4.1 Pelota is required for the epidermal barrier acquisition

The epidermal permeability barrier is a specialized structure that protects the skin from dehydration, entry of chemical or infectious agents, thereby it is essential for the extra-uterine life. Formation of the permeability barrier is a highly patterned process that begins at E16 in the mouse and is completed by birth (Hardman et al. 1998). In the epidermis, there are multiple components, which are important for the barrier function. These components include claudin, filaggrin, proteases, ceramide and desmoglein (Table 1). When properly functioning, this layer prevents water loss and provides a barrier to epidermal invasion of allergens and bacteria (Hogan et al. 2012).

Several mouse models with mutations in the genes of the stratum corneum lead to disruption of the epidermal barrier and development of skin disorders resulting in neonatal lethality. Further reports showed that defects in proteins, which are involved in lipid transport and secretion, affect as well the epidermal permeability barrier function (Segre 2003; Leyvraz et al. 2005; Herrmann et al. 2005).

Table 1. Functions of epidermal barrier components (Adapted from Hogan et al. 2012).

Barrier component	Type	Function
Claudin	Tight junction protein	Prevention of water loss
Filaggrin	Protein	Keratin-filament-aggregation.
Keratins1,10	Protein	keratin network of suprabasal keratinocytes
Transglutaminase1	Protein	Cornified cell envelope formation.
lipoxygenase3, 12R-lipoxygenase, CYP4F22, ichthyin and steroid sulfatase	Lipid	Formation of intercellular lipid layers.
ABCA12	Lipid	Lipid transport in lamellar ranules.
Skin protease inhibitors (SPINK)	Protein	Prevention of protease activity in filaggrin and ceramide production.
Ceramide	Lipid	Contribution to skin permeability barrier and epidermal differentiation
Desmoglein	Desmosome formation	Prevention of water loss
Involucrin/envoplakin/periplakin	Scaffolding protein	Structural components of epidermal barrier

The present study showed that the expression pattern of Pelo is prior to the skin barrier development indicating its relevant role in the barrier formation. Temporal loss of Pelo prior to the acquisition of a functional epidermal barrier results in neonatal lethality. *Pelo* mutant embryos died within 6 hours of cesarean section, presumably because of increased transepidermal water loss. This assumption was proved by dye penetration assay, which revealed intense penetration of toluidine blue dye through the epidermis of *Pelo* mutant embryos. Histologically, the *Pelo*-null epidermis showed thickening in some regions as a result of increased proliferation rate of the epidermal stem cells.

Defects in the epidermal differentiation or cornification result in diverse clinical disorders which are classified as ichthyosis. The perturbation in the balance between epidermal proliferation and differentiation does typically result in barrier deficiency (Serge 2006). Severe congenital ichthyosis are mainly due to mutations in genes encoding proteins that are involved in the synthesis and transport of lipids and that regulate the expression and maturation of structural proteins of the CE (Richard 2004). To date, the genes identified and found to be the cause for ichthyosis in human patients are shown in Table 2. Most ichthyosis phenotypes mentioned below exhibit a primary abnormality in the stratum corneum and associated with the barrier dysfunction (Smith et al. 2006; Akiyama 2011).

Table 2. Genetic causes of epidermal barrier defects in Human ichthyosis (Adapted from Akiyama 2011)

Barrier defect	Human disease	Molecule	Gene	Inheritance
Keratin network and keratohyalin granules	Ichthyosis vulgaris	Filaggrin (profilaggrin)	*FLG*	ASD
	Epidermolytic ichthyosis	Keratin 1	*KRT1*	AD
	Epidermolytic ichthyosis	Keratin 10	*KRT10*	AD
	Superficial epidermolytic ichthyosis	keratin 2	*KRT2*	AD
Cornified cell envelope	CIE/LI	TGase 1	TGM1	AR
Intercellular lipid layers	Harlequin ichthyosis	ABCA12	*ABCA12*	AR
	LI or CIE	lipoxygenase-3	ALOXE3	AR
	LI or CIE	12R-lipoxygenase	ALOX12B	AR

AD, autosomal dominant; AR, autosomal recessive; ASD, autosomal semidominant; CIE, Congenital ichthyosiform erythroderma; LI, Lamellar ichthyosis.

Profilaggrin is a heavily phosphorylated protein that is stored in keratohyalin granules of granular cells (Dale et al. 1985). The phosphorylated character of profilaggrin is thought to prevent its premature processing to filaggrin monomers. Thus, only dephosphorylated filaggrin monomers have keratin-filament-aggregating properties (Lonsdale-Eccles et al. 1982). The

phosphorylation sites in the profilaggrin are mainly located in the linker peptides between filaggrin repeats and considered to be the recognition sites of cleavage enzymes (Sandilands et al. 2009). Multiple kinases including AKT, protein kinase A/protein kinase G/protein kinase C (AGC), PKC and CAMK2 have been identified to be responsible for the post-translational phosphorylation of profilaggrin (Figure 19). A general decrease in phosphorylation of profilaggrin is thought to be required before its proteolytic processing into filaggrin monomers (Resing et al. 1993). The monomeric filaggrin is then secreted into the transitional zone between the granular and cornified layers, where it is involved in the assembly and cross-linking of keratin filaments (Dale et al. 1978). Analysis of *Pelo*-deficient skin revealed abnormal distribution of filaggrin-immunoreactive staining in the epidermal layers, absence of filaggrin monomers and enlarged keratohyalin granules in granular cells of mutant epidermis. These findings indicate that Pelo directly or indirectly regulates the processing of profilaggrin into filaggrin monomers during terminal differentiation of corneocytes and that is the main underlying cause for the barrier disruption.
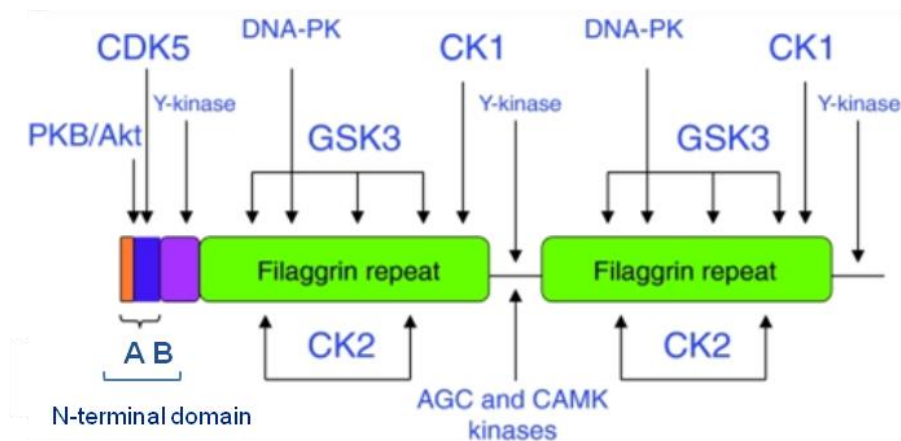
Figure 19. Schematic illustration of Protein kinases that might target profilaggrin and the predicted sites of phosphorylation. PKB/Akt, protein kinase B; CDK5, cyclin-dependent kinase 5; Y-kinase, tyrosine kinase; DNA-PK, DNA-dependent protein kinase; GSK3, glycogen synthase kinase 3; AGC/CAMK kinases, members of the AGC and CAMK kinase families (Adapted from Sandilands et al. 2009).

Analysis of different mouse models with ichthyosis revealed that either mutations in genes encoding for profilaggrin or protein involved in its proteolytic processing are linked to alterations in barrier integrity (Leyvraz et al. 2005; List et al. 2003; Fallon et al. 2009; Hoste et al. 2011). The most striking examples are the mice lacking the serine proteases matriptase (MT-SP1) (List et al. 2003) or prostasin (*Prss8*) (Leyvraz et al. 2005). Both the matriptase- and prostasin-deficient mice show impaired development of the epidermis, which is accompanied by a defective skin barrier function that results in neonatal lethality. Both mice show defects in the profilaggrin-to-filaggrin processing pathway.

For more characterization of the skin barrier defect in *Pelo*-null embryos, we evaluated the expression pattern of, *Grainy head–like 3* (*Grhl3*), *Transglutaminase 1* (*Tgase1*) and *Kruppel like factor 4* (*Klf4*) genes. These genes encode transcription factors and structural proteins that have critical role in barrier establishment. Mice lacking *Grhl3* fail to form an adequate skin barrier and die at birth due to dehydration. These defects are resulted in part, to diminished expression of a *Grhl3*-targeted gene, *Tgase 1*, which encodes a key enzyme involved in cross-linking of epidermal structural proteins and lipids into the cornified envelope. Additionally, Ting et al. (2005a) identified defect in the extracellular lipid processing as well as altered lamellar lipid architecture. There was a marked similarity between mice lacking *Grhl3* and *Klf4*-deficient animals (Ting et al. 2005b). Our expression analysis showed significant attenuated levels of *Klf4, Grhl3* and *Tgase1* in *Pelo*-deficient epidermis compared to the control during and after barrier formation. Therefore, it is of interest to address the relationship between Pelo and these epidermal barrier-related genes.

The consequence of Pelo deletion in the postnatal and adult life revealed that the perturbation of epidermal barrier function manifested by dermal infiltration of immune cells, epidermal hyperplasia and defective terminal differentiation of keratinocytes. Similar phenotype was

observed upon topical deletion of *Pelo* in the tail providing evidence that the barrier defect is rather a skin-autonomous effect.

4.2 Pelo regulates BMP and PI3K/AKT signaling pathways during barrier development

Many reports indicate the essential role of PI3K/AKT signaling in the barrier formation. O'Shaughnessy et al. (2009) found that a 'pulse' of AKT activity is coincident with the barrier acquisition in the mouse embryo. Another study from the same group showed that Akt activation is prerequisite for HspB1 intracellular relocation. HspB1 transport to the keratohyalin granules and its association with keratin filaments is probably necessary for processing of critical SC proteins like filaggrin (O'Shaughnessy et al. 2007). As mentioned above, AKT is suggested to be one of the Protein kinases that might target Profilaggrin (Sandilands et al. 2009).

The BMP pathway is another important pathway involved in the skin development. Botchkarev and Sharov (2004) described the expression pattern of type I BMPreceptors (BMPR-IA and BMPR-IB) in the basal and the suprabasal layers the epidermis respectively. These results indicate the relevant role of BMP signaling pathway in the epidermal development. Moreover, elevated activity of BMP signaling in the epidermis leads to enhanced K6 expression, increase cell proliferation rate and affect the filaggrin expression (Yu et al. 2010).

Previous reports have revealed that Pelo mediates many cellular processes through regulation of BMP and PI3K/AKT signaling pathways (Raju et al. 2015; Nyamsuren et al. 2014; Pedersen et al. 2014). Considering these knowledge, it was very important to emphasize the presence of crosstalk between *Pelo* and these two signal pathways during the barrier development. Expression pattern of Pelo during epidermal barrier formation showed similar kinetics to the activity levels of PI3K/AKT and BMP signaling pathways. Further results showed a significant elevation in the activity of both signaling pathways in the absence of Pelo, leading us to the

conclusion that Pelo negatively regulates BMP and PI3K/AKT signaling pathways during development of the epidermal barrier. Moreover, in vitro studies on control and mutant skin explants showed that inhibition of PI3K/AKT signaling resulted in a significant decrease in the levels of pAKT, which leads to impaired development of the SC in both control and mutant skin explants. These results corresponds to the findings of Peng et al. (2003), which showed that the disruption of the development of the SC and subsequent neonatal lethality were a result of attenuated PI3K/AKT activity in double null mice *Akt1* and *Akt2*. Although the levels of pAKT in mutant skin are being attenuated by LY294002-treatment, the development of epidermis was not restored. These results suggest that loss of Pelo may affect other signaling pathway(s) necessary for normal skin development. One of the most striking observations was the increase in the pSmad expression levels upon attenuation of pAKT by LY294002-treatment highlighting a relationship between BMP and PI3K/AKT signaling in skin development. Recently, BMP has been found to be a regulator of PI3K/AKT pathway during the development of different tissues (Ghosh-Choudhury et al. 2002; He et al. 2004; Sui et al. 2009). Based on these findings, we assumed that Pelo either directly or indirectly modulates BMP activity, which subsequently regulates PI3K/AKT signaling. This assumption was further confirmed by decrease in the levels of pSMAD and pAKT upon treatment of the skin explants with BMP antagonist Noggin. The restoration of epidermal permeability barrier in the mutant explants after attenuation of PI3K/AKT activity upon Noggin treatment suggest that increased AKT activity might be the cause of the impaired processing of profilaggrin .

To date the cross link between AKT and profilaggrin processing is not completely understood. A general decrease in phosphorylation levels of profilaggrin is thought to be required before its being processed into filaggrin monomers (Resing et al. 1993). PI3K/AKT signaling mediates the phosphorylation of many proteins including proteins that are involved in epidermal barrier

acquisition (O'Shaughness et al. 2007; O'Shaughnessy et al. 2009). Regarding this knowledge, we suggest that the significant elevation of pAKT in *Pelo*-depleted epidermis might counteract the dephosphorylation of profilaggrin and its processing.

We showed that the defective barrier function in *Pelo*-deficient mice is associated with a significant increase in cell proliferation in the basal layer of epidermis and defect in the terminal differentiation of keratinocytes. The defect in the between differentiation and proliferation might be responsible for the perturbation of epidermal barrier acquisition. Certainly, it is still highly questionable; How Pelo modulates the activities of both signaling pathways during epidermal barrier development?

In conclusion, our results point out that Pelo is a novel modulator of the BMP-PI3K/AKT signaling axis which promotes the maturation of profilaggrin to ensure epidermal barrier formation.

4.3 Do *PELO* mutations in humans cause Ichthyosis Vulgaris?

Ichthyosis vulgaris (IV) is one of the most common types of ichthyosis with an estimated incidence of 1 in 250-1000 births (Bremmer et al. 2008). Ichthyosis vulgaris is inherited in a semidominant manner with 83–96% penetrance (Oji et al. 2009). Clinically, IV is characterized by xerosis, scaling, keratosis, palmar and plantar hyperlinearity, with a strong predisposition to atopic disorders. Loss-of-function mutation in the *FLG* is identified as one of the major cause for IV (Sandilands et al. 2007).

Chen et al. (2008) evaluated a cohort of eight unrelated Singaporean Chinese IV patients. One Patient out of eight exhibited a severe IV phenotype and showed complete absence of filaggrin staining, but no mutation was detected. Another study found that *FLG* null mutations were present in 74% of 54 patients with isolated IV and 43% of 116 patients with AD-associated IV.

All six patients with AD with or without *FLG* mutations were demonstrated to suffer from epidermal barrier dysfunction (Li et al. 2013). The authors speculated that, it is possible that IV patients without filaggrin mutations could have mutations in another unknown gene that plays a critical role in the regulation of filaggrin expression, leading to the ichthyosiform phenotype.

Considering this knowledge from the literature and from our study on the novel role of Pelo in maturation of profilaggrin, we theorize the importance of screening for *PELO* mutations in patients with isolated IV and atopic dermatitis-associated IV whom do not show any mutations in the *FLG*. We expect that *PELO* null mutations will lead to miscarriage as we showed the importance of in *Pelo* early embryonic development and inner cell mass differentiation (Adham et al. 2003; Nyamsuren et al. 2014). We speculate that hypomorphic mutations in PELO could lead to ichthyosis disease. Patients with well-characterized mutations can be permanently cured using the ex-vivo gene therapy. Droz-Georget Lathion et al. (2015) created a new strategy for a safe ex-vivo gene therapy that permits transplantation of a clonal population of genetically corrected autologous stem cells that meet stringent selection criteria and the principle of precaution. The authors chose the Human epidermal stem cells as a good model to establish their strategy because the human epidermal stem cells expands ex vivo efficiently and hence produce a large progeny from a single stem cell (Gallico et al, 1984). Moreover, they could be transduced efficiently by means of recombinant retrovirus to produce the protein of interest (Warrick et al. 2012). This can open a new hope for IV patients to have a safe and homogenous medicinal product.

4.4 Pelota is required for self-renewal and differentiation of embryonic stem cells

Numerous studies have attempted to uncover the basic biology of the ESC and delineate mechanisms of pluripotency. However, many interesting challenges must be met in order to further understand the basic regulation of these cells. The current study introduced *Pelo* as a master regulator for a coordinated network of signaling pathways in stem cell pluripotency and differentiation. Here we report that *Pelo*-null ESCs maintain the pluripotency state under differentiating culture conditions.

Previous studies in our group showed that Pelo deficiency did not markedly affect the self-renewal of ESCs or their capacity to differentiate in teratoma assays. However, their differentiation into ExEn in the embryoid bodies was severely compromised. The failure of *Pelo*-null ESCs to silence the pluripotency-related genes during the EB formation was attributed to failed signals from surrounding ExEn that induce the differentiation program (Nyamsuren et al. 2014). That was also the case in Dido3-deficient EB where the loss of Dido3 expression delays primitive endoderm formation and maintains pluripotency (Fütterer et al. 2012).

Using defined monolayer culture conditions, we demonstrated that *Pelo*-null ESCs retain their capacity to form undifferentiated dome shaped colonies and maintain expression of pluripotent markers under differentiation conditions. Our analysis of $Pelo^{\Delta/-}$ ESCs revealed high levels of pAKT compared to control $Pelo^{F/-}$. Because previous studies have demonstrated the critical roles of PI3K/AKT in the self-renewal of ESCs (Takahashi et al. 2005; McLean 2007), we assumed that activation of AKT signaling supports the pluripotency of mutant ES cells and hereby affect the differentiation. However, addition of Wortaminin, a PI3K inhibitor, in cultures did not induce differentiation of the mutant ESCs judged by the ESCs morphology and with the persistent

expression of the pluripotent marker Oct4. These findings led us to determine other factors apart from PI3K/AKT that can maintain the ESCs pluripotency.

On the other hand addition of Retonic acid induced complete differentiation of *Pelo*-mutant ESCs. RA is known in the literature as a potent differentiation agent. In contrast, retinol, which is the precursor of RA, was found to maintain the ESC self-renewal by elevating the expression of Nanog (Chen et al. 2007). Later, it was described that retinol maintains the pluripotency of ES cells through activation of PI3K/AKT in an insulin-like growth factor I (IGF-1) receptor/insulin receptor substrate 1(IRS-1)-dependent manner (Chen and Khillan 2010). Analysis of ESCs revealed that these cells are unable to metabolize retinol to retinoic acid due to lack of retinol metabolizing machinery in the ESCs. This result was further supported by the observations that addition of retinoic acid leads to their complete differentiation (Chen and Khillan 2008). In absence of LIF, ESCs are capable of synthesizing active retinoids (4-hydroxyretinol and 4-oxoretinol) from retinol. These retinoids can activate transcription through the retinoic acid receptors (RARs), leading to ESCs differentiation without forming retinoic acid (Lane et al. 1999). Based on these information, we speculate that $Pelo^{\Delta/-}$ ESCs fail to metabolize retinol to active retinoids in differentiating culture conditions. Therefore, accumulation of retinol in *Pelo*-mutant ESCs may be responsible for maintaining the ESCs pluripotency. To prove this speculation we checked the expression of *stra8* gene, as its promoter region contains RA response elements, suggesting that RA could be turning on this gene directly (Zhou et al. 2008). Expression analysis of *stra8* mRNA in $Pelo^{\Delta/-}$ ESCs were significantly lower than that in control ESCs in undifferentiated state as well as after inducing differentiation. These results confirm our assumption that retinol metabolism in *Pelo*-mutant ESCs is affected.

Recent study by Obrochta et al. (2015) linked the activity of Foxo1to retinol metabolism. Thus, cis-acting elements of Foxo1 have been identified in the promoters of genes associated with retinoid metabolism, including retinol dehydrogenases (*RDH*). The authors showed that enhancing the activity of PI3K/AKT signaling pathway decreases the transcription activity of Foxo1, followed by repression of *RDH* transcription, leading to decrease in retinoic acid synthesis from retinol.

Although AKT activity enhance the nuclear export of phosphorylated FOXO proteins and hereby inhibit their transcriptional activity (Figure 20) (Van den Berg & Burgering 2011), our protein blot analysis revealed a significant increase in the levels of nuclear Foxo1in *Pelo*-mutant ESCs. This result corresponds to Zhang et al. (2011) findings, which highlighted the essential role of Foxo1 in maintaining ESCs pluripotency through direct control of Oct4 and Sox2 expression. Despite enhanced activity of PI3K\AKT signaling pathway, Foxo1 was nuclear and transcriptionally active concluding that PI3K\AKT signaling pathway is not the predominant regulator of Foxo1 in ESCs. Other study presumed that Foxo1 inhibition by pAKT is overridden by other signaling pathways (Yamagata et al. 2008).
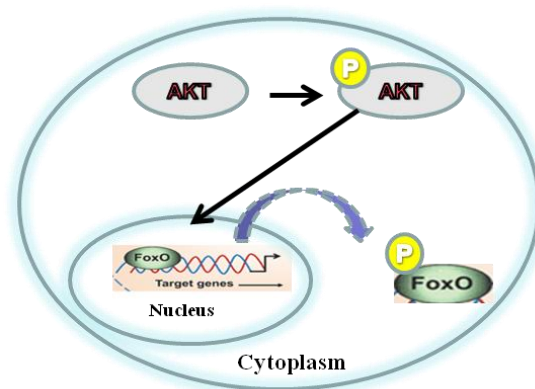
Figure 20. Model of FOXO regulation by PI3K\AKT signaling pathway. Phosphorylated AKT phosphorylates FOXO transcription factors leading to nuclear export and inactivation of transcriptional activity by FOXO.

Therefore, we were interested to have a more detailed insight about the effect of increased transcription activity of Foxo1 in *Pelo*-null ESCs. The association of Foxo proteins with β-catenin was elucidated by Almeida et al. (2007). The same group in 2013 provided genetic evidence that FOXOs do indeed bind with β-catenin diverting the limited pool of β-catenin from Wnt/TCF to FOXO mediated transcription resulting in attenuation of β-catenin/TCF transcription in murine osteoblast progenitors (Figure 21). Generally Wnt binding to the Frizzled-LRP5/6 receptor complex halting the proteolytic destruction of β-catenin, which then moves into the nucleus where it binds to and activates the T cell factor (TCF) lymphoid-enhancer binding factor (LEF) transcription factors and regulates the expression of Wnt-target genes (Figure 21) (Rodda and McMahon 2006). The binding of FOXOs to β-catenin mechanism, restrain the proliferative effects of Wnt signaling. Suppression of the proliferative β-catenin/TCF transcriptional signal by FOXOs is probably a defense mechanism against diverse stress stimuli in many tissues, as evidenced by the increased association of β-catenin with FOXOs in H2O2-treated bone and colon cancer cells (Hoogeboom et al. 2008).
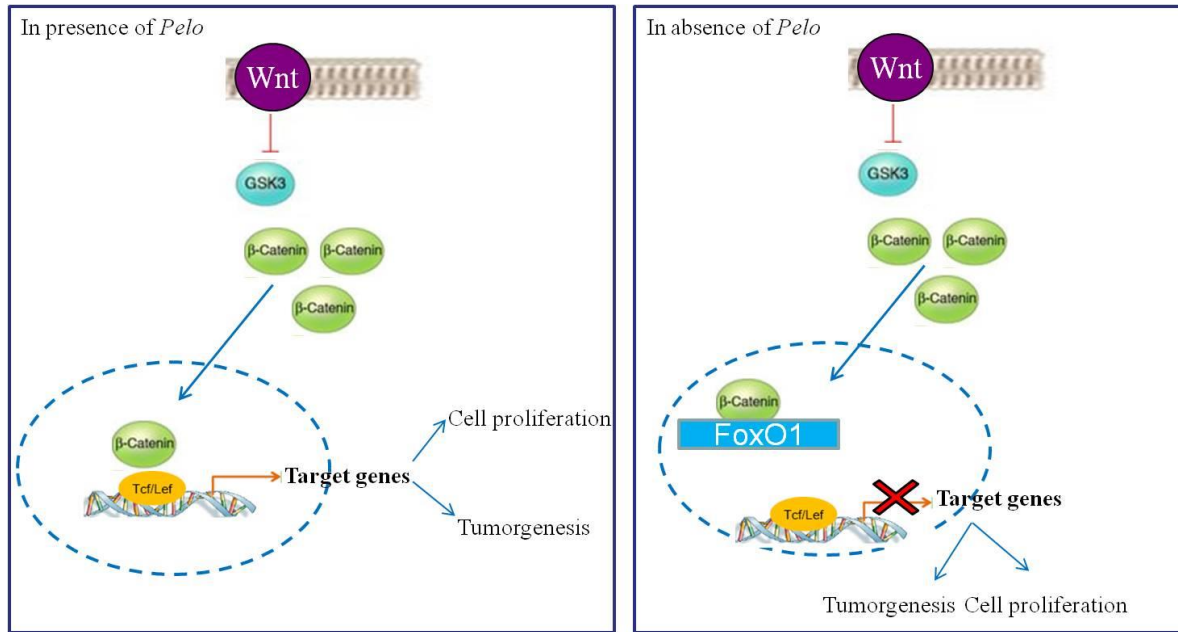
Figure 21. Model for binding of FOXOs to β-catenin in ESCs. In presence of *Pelo* (right panel) binding of Wnt ligand to a Frizzled/LRP-5/6 receptor complex (right panel) leads to stabilization of hypophosphorylated β-catenin, which interacts with TCF/LEF proteins in the nucleus and regulates Wnt-target genes transcription. In the absence of *Pelo* (left panel), β-catenin tends to bind to nuclear Foxo1 diverting β-catenin from β-catenin/TCF target genes transcription (Adapted from Sun 2010).

In Regards to these literatures and to our results that showed increased levels of Foxo1 in *Pelo*-null ESCs. We hypothesized that in ESCs upon *Pelo* deletion Foxo1 diverts β-catenin from TCF/LEF leading to attenuation of β-catenin/TCF transcription activity and altering Foxo-mediated transcription (Figure 22). This hypothesis is supported by our pervious results that related the decreased proliferative capacity of *Pelo*-mutant ESCs to low levels of c-Myc, a candidate for β-catenin/TCF transcription activity, as well as by the significant decrease of TCF/LEF transcription activity in *Pelo*-mutant ESCs as judged by TOP/FOP-FlASH reporter assay.
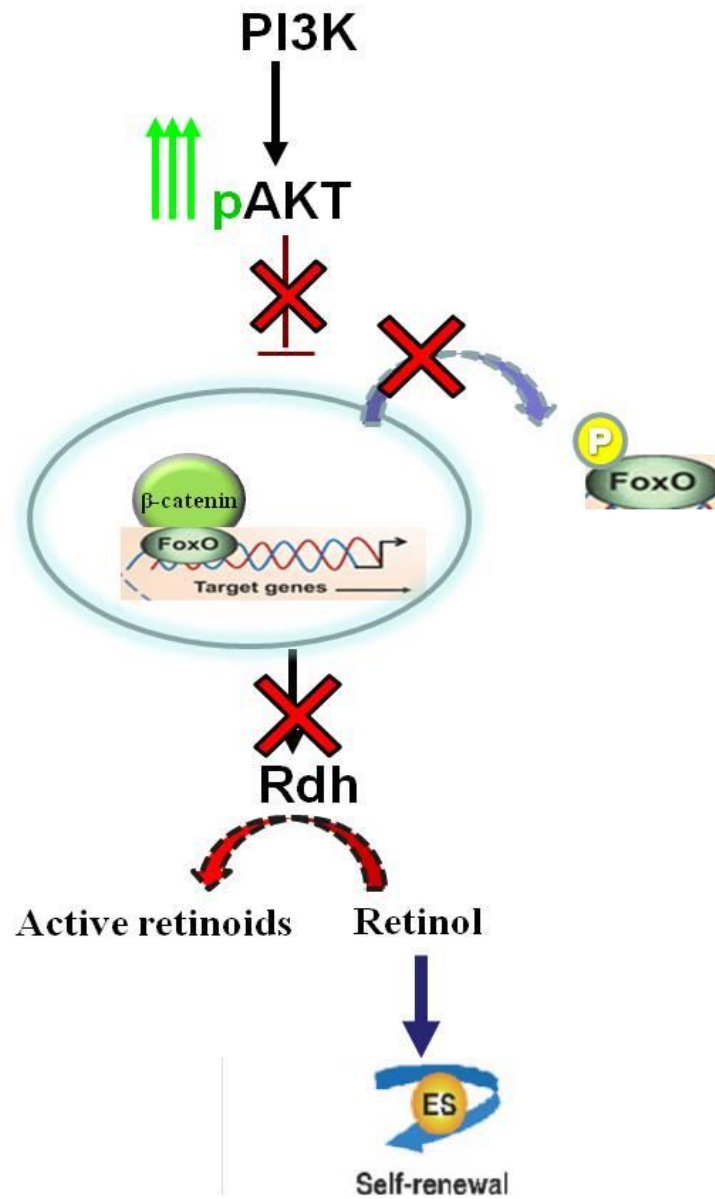
Figure 22. Model of Mechanisms that contribute to *Pelo*-null ESCs pluripotency. *Pelo* deletion increases AKT activity, Foxo1escapes the inhibitory effect of pAKT and remain nuclear. Activity of Foxo1 maintains the ESCs pleuripotency and decreases β-catenin/TCF-mediated transcription. This disrupts the RDH expression and thereby blocks the metabolism of retinol to active retinoids, which induce ESCs differentiation in absence of LIF. Retinol also contributes to ESCs pluripotency and lack of differentiation. (Adapted from Obrochta et al. 2015).

5. Summary

The skin acts as a first protective barrier that diminishes the fluid loss from the body and prevents the entry of toxic and pathogenic agents. Defect in the formation of the epidermal barrier results in neonatal lethality and increased susceptibility to skin inflammation. Here, we show that temporal depletion of Pelota (Pelo) during embryonic development disrupts the acquisition of epidermal barrier. The defective function of epidermal barrier in *Pelo*-deficient mice is a result of failed processing of profilaggrin into filaggrin monomers, which promote the formation of protective epidermal layer. Expression analysis revealed that the expression pattern of Pelo correlates with the epidermal barrier formation and resemble that of pSmad and pAKT. Further experiments showed that Pelo negatively regulates BMP-PI3K/AKT signaling pathways. Hence activation of BMP-PI3K/AKT was the underlying cause for the perturbed function of *Pelo*-deficient epidermis.

Inhibition of PI3K/AKT and BMP signaling pathways by addition of PI3K inhibitor and Noggin respectively, in organotypic culture of mutant and control skin explants revealed that attenuated activity of PI3K/AKT did not significantly affect the BMP activity. In contrast, inhibition of BMP signaling resulted in a significant decrease in the PI3K/AKT activity in mutant skin and interestingly the restoration of the profilaggrin processing and the epidermal barrier function.

In adult mice, deletion of *Pelo* resulted in epidermal hyperproliferation, abnormal differentiation of keratinocytes and cutaneous inflammation. These phenotypes are often associated with epidermal barrier dysfunction. To determine whether these symptoms are due to systemic immune-system disorder or a result of affected skin barrier, *Pelo* was topically deleted in a small region of the tail skin. Histological analyses revealed that hyperkeratosis and increased infiltration of mast cells were only restricted to the topically *Pelo*-deficient skin region and the

other skin areas were completely normal. Additionally, our results showed the perturbation of the epidermal barrier function in *Pelo*-null skin explants grown *in vitro* providing strong evidence that the barrier defect was not due to systemic effect of *Pelo* deletion, but due to skin-autonomous effect.

These results point out that Pelo is a novel modulator of the BMP-PI3K/AKT signaling axis which promotes the maturation of profilaggrin to ensure epidermal barrier formation.

In the second part of the study, we investigated the molecular causes for attenuated rate of cell proliferation and impaired differentiation of *Pelo*-deficient ESCs. We found that the elevated activity of PI3K/AKT signaling is not the cause for impaired differentiation of *Pelo*-null ESCs. Despite the enhanced activity of PI3K/AKT in *Pelo*-null ESCs, Foxo1 escapes the inhibitory effect of PI3K/AKT signaling and retain in the nucleus. Nuclear Foxo1 tends to divert β-catenin from binding TCF and hereby restrain the WNT/TCF activity.

Induction of ESC differentiation by retinoic acid (RA) led us to suggest that retinol metabolism in *Pelo* mutant ESCs is disrupted. As *RDH* is one targets of Foxo1, we assumed that the binding of Foxo1to β-catenin on one hand decreased the proliferative effect of Wnt signaling pathway and on the other hand altered the Foxo1 transcription activity. Therefore, the *RDH* transcription was affected resulting in defect in retinol metabolism to active retinoids, and probably this was the underlying cause for impaired differentiation of *Pelo*-mutant ESCs in absence of LIF.

Extending the study on role of *Pelo* in ESCs self-renewal and differentiation would add valuable information about the role of PELO during early embryonic development, Moreover this knowledge may be used for improving somatic cell reprogramming as well.

6. References

Adham IM, Sallam MA, Steding G, Korabiowska M, Brinck U, Hoyer-Fender S, Oh C, Engel W (2003): Disruption of the pelota gene causes early embryonic lethality and defects in cell cycle progression. Mol Cell Biol <u>23</u>, 1470-1476

Akiyama M (2011): Updated molecular genetics and pathogenesis of ichthiyoses. Nagoya J Med Sci <u>73</u>, 79-90

Almeida M, Han L, Martin-Millan M, O'Brien CA, Manolagas SC (2007): Oxidative stress antagonizes Wnt signaling in osteoblast precursors by diverting beta-catenin from T cell factor- to forkhead box O-mediated transcription. J Biol Chem <u>282</u>, 27298-27305

Blanpain C, Fuchs E (2006): Epidermal stem cells of the skin. Annu Rev Cell Dev Biol <u>22</u>, 339-373

Boguniewicz M, Leung DY (2011): Atopic dermatitis: a disease of altered skin barrier and and immune dysregulation. Immunol Rev <u>242</u>, 233-246

Botchkarev VA, Sharov AA (2004): BMP signaling in the control of skin development and hair follicle growth. Differentiation <u>72</u>, 512-526

Bremmer SF, Hanifin JM, Simpson EL (2008): Clinical detection of ichthyosis vulgaris in an atopic dermatitis clinic: implications for allergic respiratory disease and prognosis. J Am Acad Dermatol <u>59</u>, 72-78

Brunet A, Bonni A, Zigmond MJ, Lin MZ, Juo P, Hu LS, Anderson MJ, Arden KC, Blenis J, Greenberg ME (1999): Akt promotes cell survival by phosphorylating and inhibiting a Forkhead transcription factor. Cell <u>96</u>, 857-868

Burnicka-Turek O, Kata A, Buyandelger B, Ebermann L, Kramann N, Burfeind P, Hoyer-Fender S, Engel W, Adham IM (2010): Pelota interacts with HAX1, EIF3G and SRPX and the resulting protein complexes are associated with the actin cytoskeleton. BMC Cell Biol <u>11</u>, 28

Castrillon DH, Gönczy P, Alexander S, Rawson R, Eberhart CG, Viswanathan S, DiNardo S, Wasserman SA (1993): Toward a molecular genetic analysis of spermatogenesis in Drosophila melanogaster: characterization of male-sterile mutant generated by single E-element mutagenesis. Genetics <u>135</u>, 489-505

Chan LS, Robinson N, Xu L (2001): Expression of interleukin-4 in the epidermis of transgenic mice results in a pruritic inflammatory skin disease: an experimental animal model to study atopic dermatitis. J Invest Dermatol <u>117</u>, 977-983

Chen H, Ho JC, Sandilands A, Chan YC, Giam YC, Evans AT, Lane EB, McLean WH (2008): Unique and recurrent mutations in the filaggrin gene in Singaporean Chinese patients with ichthyosis vulgaris. J Invest Dermatol <u>128</u>, 1669-1675

Chen L, Khillan JS (2008): Promotion of feeder-independent self-renewal of embryonic stem cells by retinol (vitamin A). Stem Cells <u>26</u>, 1858-1864

Chen L, Khillan JS (2010): A novel signaling by vitamin A/retinol promotes self renewal of mouse embryonic stem cells by activating PI3K/Akt signaling pathway via insulin-like growth factor-1 receptor. Stem Cells 28, 57-63

Chen L, Yang M, Dawes J, Khillan JS (2007): Suppression of ES cell differentiation by retinol (vitamin A) via the overexpression of Nanog. Differentiation 75, 682-693

Chen L, Muhlrad D, Hauryliuk V, Cheng Z, Lim MK, Shyp V, Parker R, Song H (2010): Structure of theDom34-Hbs1 complex and implications for no-go decay. Nat Struct Mol Biol 17, 1233-1240

Cole SE, LaRiviere FJ, Merrikh CN, Moore MJ (2009): A convergence of rRNA and mRNA quality control pathways revealed by mechanistic analysis of nonfunctional rRNA decay. Mol Cell 34, 440-450

Dale BA, Holbrook KA, Steinert PM (1978): Assembly of stratum corneum basic protein and keratin filaments in macrofibrils. Nature 276, 729-731

Dale BA, Holbrook KA, Kimball JR, Hoff M, Sun TT (1985): Expression of epidermal and filaggrin during human fetal skin development. J Cell Biol 101, 1257-1269

Davis L, Engebrecht J (1998): Yeast dom34 mutants are defective in multiple developmental pathways and exhibit decreased levels of polyribosomes. Genetics 149, 45-56

Demehri S, Morimoto M, Holtzman MJ, Kopan R (2009): Skin-derived TSLP triggers progression from epidermal-barrier defects to asthma. PLoS Biol 7, 1000067

Doma MK, Parker R (2006): Endonucleolytic cleavage of eukaryotic mRNAs with stalls in translation elongation. Nature 23, 561-564

Droz-Georget Lathion S, Rochat A, Knott G, Recchia A, Martinet D, Benmohammed S, Grasset N, Zaffalon A, Besuchet Schmutz N, Savioz-Dayer E et al. (2015): A single epidermal stem cell strategy for safe ex vivo gene therapy. EMBO Mol Med 27, 380-393

Eberhart CG, Wasserman SA (1995). The pelota locus encodes a protein required for meiotic cell division: an analysis of G2/M arrest in Drosophila spermatogenesis. Development 121, 3477-3486

Essers MA, de Vries-Smits LM, Barker N, Polderman PE, Burgering BM, Korswagen HC (2005): Functional interaction between beta-catenin and FOXO in oxidative stress signaling. Science 308, 1181-1184

Fallon PG, Sasaki T, Sandilands A, Campbell LE, Saunders SP, Mangan NE, Callanan JJ, Kawasaki H, Shiohama A, Kubo A et al. (2009): A homozygous frameshift mutation in the mouse Flg gene facilitates enhanced percutaneous allergen priming. Nat Genet 41, 602-608

Fuchs E (2007): Scratching the surface of skin development. Nature 445, 834-842

Fütterer A, Raya A, Llorente M, Izpisúa-Belmonte JC, de la Pompa JL, Klatt P, Martínez-A C (2012): Ablation of Dido3 compromises lineage commitment of stem cells in vitro and during early embryonic development. Cell Death Differ 19, 132-143

Gallico GG 3rd, O'Connor NE, Compton CC, Kehinde O, Green H (1984): Permanent coverage of large burn wounds with autologous cultured human epithelium. N Engl J Med 311, 448-451

Ghosh-Choudhury N, Abboud SL, Nishimura R, Celeste A, Mahimainathan L, Choudhury GG (2002): Requirement of BMP-2-induced phosphatidylinositol 3-kinase and Akt serine/threonine kinase in osteoblast differentiation and Smad-dependent BMP-2 gene transcription. J Biol Chem 277, 33361-33368

Graille M, Chaillet M, van Tilbeurgh H (2008): Structure of yeast Dom34: a protein related to translation termination factor Erf1 and involved in no-go decay. J Biol Chem 283, 7145–7154

Gudas LJ (1994): Retinoids and vertebrate development. J Biol Chem 269, 15399-15402

Hardman MJ, Sisi P, Banbury DN, Byrne C (1998): Patterned acquisition of skin barrier function during development. Development 125, 1541-1552

He XC, Zhang J, Tong WG, Tawfik O, Ross J, Scoville DH, Tian Q, Zeng X, He X, Wiedemann LM, et al. (2004): BMP signaling inhibits intestinal stem cell self-renewal through suppression of Wnt-beta-catenin signaling. Nat Genet 36, 1117-1121

Herrmann T, Gröne HJ, Langbein L, Kaiser I, Gosch I, Bennemann U, Metzger D, Chambon P, Stewart AF, Stremmel W (2005): Disturbed epidermal structure in mice with temporally controlled fatp4 deficiency. J Invest Dermatol 125, 1228-1235

Hoffjan S, Stemmler S (2007): On the role of the epidermal differentiation complex in ichthyosis vulgaris, atopic dermatitis and psoriasis. Br J Dermatol 157, 441-449

Hogan MB, Peele K, Wilson NW (2012): Skin barrier function and its importance at the start of the atopic march. J Allergy (Cairo) 2012, 901940

Hoogeboom D, Essers MA, Polderman PE, VoetsE, Smits LM, Burgering BM (2008): Interaction of FOXO with beta-catenin inhibits beta-catenin/T cell factor activity. J Biol Chem 283, 9224–9230

Hoste E, Kemperman P, Devos M, Denecker G, Kezic S, Yau N, Gilbert B, Lippens S, De Groote P, Roelandt R et al. (2011). Caspase-14 is required for filaggrin degradation to natural moisturizing factors in the skin. J Invest Dermatol 131, 2233-2241

Irvine AD, McLean WH, Leung DY (2011): Filaggrin mutations associated with skin and allergic diseases. N Engl J Med 365, 1315-1327

Kalinin AE, Kajava AV, Steinert PM (2002): Epithelial barrier function: assembly and structural features of the cornified cell envelope. Bioessays 24, 789-800

Kan L, Liu Y, McGuire TL, Bonaguidi MA, Kessler JA (2011): Inhibition of BMP signaling in P-Cadherin positive hair progenitor cells leads to trichofolliculoma-like hair follicle neoplasias. J Biomed Sci 18, 92

Khillan JS (2014): Vitamin A/retinol and maintenance of pluripotency of stem cells. Nutrients 6, 1209-1222

Kobayashi K, Kikuno I, Kuroha K, Saito K, Ito K, Ishitani R, Inada T, Nureki O (2010): Structural basis for mRNA surveillance by archaeal Pelota and GTP-bound EF1α complex. Proc Natl Acad Sci U S A 107, 17575-17579

Lane MA, Chen AC, Roman SD, Derguini F, Gudas LJ (1999): Removal of LIF (leukemia inhibitory factor) results in increased vitamin A (retinol) metabolism to 4-oxoretinol in embryonic stem cells. Proc Natl Acad Sci U S A 96, 13524-13529

Lee MY, Lim HW, Lee SH, Han HJ (2009): Smad, PI3K/Akt, and Wnt-dependent signaling pathways are involved in BMP-4-induced ESC self-renewal. Stem Cells 27, 1858-1868

Leslie NR, Downes CP (2004): PTEN function: how normal cells control it and tumour cells lose it. Biochem J 382, 1-11

Leyvraz C, Charles RP, Rubera I, Guitard M, Rotman S, Breiden B, Sandhoff K, Hummler E (2005): The epidermal barrier function is dependent on the serine protease CAP1/Prss8. J Cell Biol 170, 487-496

Li M, Cheng R, Shi M, Liu J, Zhang G, Liu Q, Yu H, Yao Z (2013): Analyses of FLG mutation frequency and filaggrin expression in isolated ichthyosis vulgaris (IV) and atopic dermatitis-associated IV. Br J Dermatol 168, 1335-1338

List K, Szabo R, Wertz PW, Segre J, Haudenschild CC, Kim SY, Bugge TH (2003): Loss of proteolytically processed filaggrin caused by epidermal deletion of Matriptase/MT-SP1. J Cell Biol 163, 901-910

Lonsdale-Eccles JD, Teller DC, Dale BA (1982): Characterization of a phosphorylated form of the intermediate filament-aggregating protein filaggrin. Biochemistry 21, 5940-5948

Iyer S, Ambrogini E, Bartell SM, Han L, Roberson PK, de Cabo R, Jilka RL, Weinstein RS, O'Brien CA, Manolagas SC, et al. (2013): FOXOs attenuate bone formation by suppressing Wnt signaling. J Clin Invest 123, 3409-3419

Martin G (1981): Isolation of a pluripotent cell line from early mouse embryos cultured in medium conditioned by teratocarcinoma stem cells. Proc Natl Acad Sci U S A 78, 7634–7638

Matsui T, Miyamoto K, Kubo A, Kawasaki H, Ebihara T, Hata K, Tanahashi S, Ichinose S, Imoto I, Inazawa J et al. (2011): SASPase regulates stratum corneum hydration through profilaggrin-to-filaggrin processing. EMBO Mol Med 3, 320-333

McLean AB, D'Amour KA, Jones KL, Krishnamoorthy M, Kulik MJ, Reynolds DM, Sheppard AM, Liu H, Xu Y, Baetge EE, Dalton S (2007): Activin a efficiently specifies definitive endoderm from human embryonic stem cells only when phosphatidylinositol 3-kinase signaling is suppressed. Stem Cells 25, 29-38

Nii T, Marumoto T, Kawano H, Yamaguchi S, Liao J, Okada M, Sasaki E, Miura Y, Tani K (2014): Analysis of essential pathways for self-renewal in common marmoset embryonic stem cells. FEBS Open Bio 4, 213-219

Nyamsuren G, Kata A, Xu X, Raju P, Dressel R, Engel W, Pantakani DV, Adham IM (2014): Pelota regulates thedevelopment of extraembryonic endoderm through activation of bone morphogenetic protein (BMP) signaling. Stem Cell Res 13, 61-74

Oatley JM, Avarbock MR, Telaranta AI, Fearon DT, Brinster RL (2006): Identifying genes important for spermatogonial stem cell self-renewal and survival. Proc Natl Acad Sci U S A. 103, 9524-9529

Obrochta KM, Krois CR, Campos B, Napoli JL (2015): Insulin regulates retinol dehydrogenase expression and all-trans-retinoic acid biosynthesis through FoxO1. J Biol Chem 290, 7259-7268

Oji V, Seller N, Sandilands A, Gruber R, Gerss J, Hüffmeier U, Hamm H, Emmert S, Aufenvenne K, Metze D et al. (2009): Ichthyosis vulgaris: novel FLG mutations in the German population and high presence of CD1a+ cells in the epidermis of the atopic subgroup. Br J Dermatol 160, 771-781

O'Shaughnessy RF, Welti JC, Cooke JC, Avilion AA, Monks B, Birnbaum MJ, Byrne C (2007): AKT-dependent HspB1 (Hsp27) activity in epidermal differentiation. J Biol Chem 282, 17297-17305

O'Shaughnessy RF, Welti JC, Sully K, Byrne C (2009): Akt-dependent Pp2a activity is required for epidermal barrier formation during late embryonic development. Development 136, 3423-3431

Oulad-Abdelghani M, Bouillet P, Décimo D, Gansmuller A, Heyberger S, Dollé P, Bronner S, Lutz Y, Chambon P (1996): Characterization of a premeiotic germ cell-specific cytoplasmic protein encoded by Stra8, a novel retinoic acid-responsive gene. J Cell Biol 135, 469-477

Paling NR, Wheadon H, Bone HK, Welham MJ (2004): Regulation of embryonic stem cell self-renewal by phosphoinositide 3-kinase-dependent signaling. J Biol Chem 279, 48063-48070

Palmer CN, Irvine AD, Terron-Kwiatkowski A, Zhao Y, Liao H, Lee SP, Goudie DR, Sandilands A, Campbell LE, Smith FJ et al. (2006): Common loss-of-function variants of the epidermal barrier protein filaggrin are a major predisposing factor for atopic dermatitis. Nat Genet 38, 441-446

Pedersen K, Canals F, Prat A, Tabernero J, Arribas J (2014). PELO negatively regulates HER receptor signaling and metastasis. Oncogene 33, 1190-1197

Peng XD, Xu PZ, Chen ML, Hahn-Windgassen A, Skeen J, Jacobs J, Sundararajan D, Chen WS, Crawford SE, Coleman KG et al. (2003): Dwarfism, impaired skin development, skeletal muscle atrophy, delayed bone development, and impeded adipogenesis in mice lacking Akt1 and Akt2. Genes Dev 17, 1352–1365

Pisareva VP, Skabkin MA, Hellen CU, Pestova TV, Pisarev AV (2011): Dissociation by Pelota, Hbs1 and ABCE1 of mammalian vacant 80S ribosomes and stalled elongation complexes. EMBO J 30, 1804-1817

Raju P, Nyamsuren G, Elkenani M, Kata A, Tsagaan E, Engel W, Adham IM (2015): Pelota mediates gonocyte maturation and maintenance of spermatogonial stem cells in mouse testes. Reproduction 149, 213-221

Resing KA, Johnson RS, Walsh KA (1993): Characterization of protease processing sites during conversion of rat profilaggrin to filaggrin. Biochemistry 32, 10036-10045

Richard G (2004): Molecular genetics of the ichthyoses. Am J Med Genet C Semin Med Genet 131, 32-44

Rodda SJ, McMahon AP (2006): Distinct roles for Hedgehog and canonical Wnt signaling in specification, differentiation and maintenance of osteoblast progenitors.Development 133, 3231-3244

Sandilands A, Terron-Kwiatkowski A, Hull PR, O'Regan GM, Clayton TH, Watson RM, Carrick T, Evans AT, Liao H, Zhao Y et al. (2007): Comprehensive analysis of the gene encoding filaggrin uncovers prevalent and rare mutations in ichthyosis vulgaris and atopic eczema. Nat Genet 39, 650-654

Sandilands A, Sutherland C, Irvine AD, McLean WH (2009): Filaggrin in the frontline: role in skin barrier function and disease. J Cell Sci 122, 1285-1294

Segre J (2003): Complex redundancy to build a simple epidermal permeability barrier. Curr OpinCell Biol 15, 776-782

Segre JA (2006): Epidermal barrier formation and recovery in skin disorders. J Clin Invest 116, 1150-1158

Shamsadin R, Adham IM, Engel W (2002): Mouse pelota gene (Pelo): cDNA cloning, genomic structure, and chromosomal localization. Cytogenet Genome Res 97, 95-99

Shoemaker CJ, Green R (2011): Kinetic analysis reveals the ordered coupling of translation termination and ribosome recycling in yeast. Proc Natl Acad Sci U S A 108, 1392-1398

Shtutman M, Zhurinsky J, Simcha I, Albanese C, D'Amico M, Pestell R, Ben-Ze'ev A (1999): The cyclin D1 gene is a target of the beta-catenin/LEF-1 pathway. Proc Natl Acad Sci U S A 96, 5522-5527

Smith FJ, Irvine AD, Terron-Kwiatkowski A, Sandilands A, Campbell LE, Zhao Y, Liao H, Evans AT, Goudie DR, Lewis-Jones S, Arseculeratne G, et al. (2006): Loss-of-function mutations in the gene encoding filaggrin cause ichthyosis vulgaris. Nat Genet. 38, 337-342

Sui X, Li D, Qiu H, Gaussin V, Depre C (2009): Activation of the bone morphogenetic protein receptor by H11kinase/Hsp22 promotes cardiac cell growth and survival. Circ Res 104, 887-895

Sun J (2010): Enteric bacteria and cancer stem cells. Cancers (Basel) 3, 285-297

Takahashi K, Murakami M, Yamanaka S (2005): Role of the phosphoinositide 3-kinase pathway in mouse embryonic stem (ES) cells. Biochem Soc Trans 33, 1522-1525

Thomson JA, Itskovitz-Eldor J, Shapiro SS, Waknitz MA, Swiergiel JJ, Marshall VS, Jones JM (1998): Embryonic stem cell lines derived from human blastocysts. Science 282, 1145-1147

Ting SB, Caddy J, Wilanowski T, Auden A, Cunningham JM, Elias PM, Holleran WM, Jane SM (2005 a): The epidermis of grhl3-null mice displays altered lipid processing and cellular hyperproliferation. Organogenesis 2, 33-35

Ting SB, Caddy J, Hislop N, Wilanowski T, Auden A, Zhao LL, Ellis S, Kaur P, Uchida Y, Holleran WM et al. (2005b): A homolog of Drosophila grainy head is essential for epidermal integrity in mice. Science 308, 411-413

Tritschler F, Eulalio A, Truffault V, Hartmann MD, Helms S, Schmidt S, Coles M, Izaurralde E, Weichenrieder O (2007): A divergent Sm fold in EDC3 proteins mediates DCPI binding and P-body targeting. Mol Cell Biol 27, 8600–8611

Tsuboi T, Kuroha K, Kudo K, Makino S, Inoue E, Kashima I, Inada T (2012): Dom34:hbs1 plays a general role in quality-control systems by dissociation of a stalled ribosome at the 3' end of aberrant mRNA. Mol Cell 46, 518-529

van den Berg MC, Burgering BM (2011): Integrating opposing signals toward Forkhead box O. Antioxid Redox Signal 14, 607-621

Wang X, McCullough KD, Franke TF, Holbrook NJ (2000): Epidermal growth factor receptor-dependent Akt activation by oxidative stress enhances cell survival. J Biol Chem 275, 14624-14631

Warrick E, Garcia M, Chagnoleau C, Chevallier O, Bergoglio V, Sartori D, Mavilio F, Angulo JF, Avril MF, Sarasin A (2012): Preclinical corrective gene transfer in xeroderma pigmentosum human skin stem cells. Mol Ther 20, 798-807

Xi R, Doan C, Liu D, Xie T (2005): Pelota controls self-renewal of germline stem cells by repressing a Bam-independent differentiation pathway. Development 132, 5365-5374

Yamagata K, Daitoku H, Takahashi Y, Namiki K, Hisatake K, Kako K, Mukai H, Kasuya Y, Fukamizu A (2008): Arginine methylation of FOXO transcription factors inhibits their phosphorylation by Akt. Mol Cell 32, 221-231

Yang F, Zhao R, Fang X, Huang H, Xuan Y, Ma Y, Chen H, Cai T, Qi Y, Xi R (2015): The RNA surveillance complex Pelo-Hbs1 is required for transposon silencing in the Drosophila germline. EMBO Rep 16, 965-74

Yoshida S, Sukeno M, Nakagawa T, Ohbo K, Nagamatsu G, Suda T, Nabeshima Y (2006): The first round of mouse spermatogenesis is a distinctive program that lacks the self-renewing spermatogonia stage. Development 133, 1495-1505

Yu X, Espinoza-Lewis RA, Sun C, Lin L, He F, Xiong W, Yang J, Wang A, Chen Y (2010): Overexpression of constitutively active BMP-receptor-IB in mouse skin causes an ichthyosis-vulgaris-like disease. Cell Tissue Res 342, 401-410

Zhang X, Yalcin S, Lee DF, Yeh TY, Lee SM, Su J, Mungamuri SK, Rimmelé P, Kennedy M, Sellers R et al. (2011): FOXO1 is an essential regulator of pluripotency in human embryonic stem cells. Nat Cell Biol 13, 1092-1099

Zhou Q, Nie R, Li Y, Friel P, Mitchell D, Hess RA, Small C, Griswold MD (2008): Expression of stimulated by retinoic acid gene 8 (Stra8) in spermatogenic cells induced by retinoic acid: an in vivo study in vitamin A-sufficient postnatal murine testes. Biol Reprod <u>79</u>, 35-42

Acknowledgment

I want to express my deep gratitude to **Prof. Dr. I. M. Adham**, for closely supervising my thesis through the entire course of my MD study and for encouraging me to participate actively in meetings and conferences. His great experience helped me to adapt into the field of molecular biology

I would like to sincerely thank **Prof. Dr. med. Dr. h. c. Wolfgang Engel**, for giving me this great chance to do my MD study in the Institute of Human Genetics, University of Göttingen and for his guidance and helpful suggestions during my MD study.

I thank my lab mates and all my institute colleagues for their friendship, advices and for the encouraging lab atmosphere they created.

Curriculum vitae

I was born in Mansoura, Eygpt on 08.12.1981 as the second child of my parents Mohamed El kenani and Magda Elshabrawy.

From 1987 till 1998, I visited the Primary and Secondary schools in Mansoura, Egypt. I passed the Secondary school final examination in 1998. From 1998 till 2004, I studied Medicine in the Faculty of Medicine, Mansoura University. In 2004, I got my Bachelor degree in Internal Medicine and General Surgery with the grade "Excellent with Honour". From 2004 till 2005, I did training courses as a rotatory internship in the Mansoura University Hospitals. In September 2005 I started my residency in the Department of Clinical Pathology. In May 2009, I got the certificate of post-graduate studies (Master degree) in Clinical Pathology with grade "Very Good". The title of my master thesis was "Breast Cancer: Current status and Future approach". Since 2009 I am an assistant lecturer in Clinical Pathology Department, Faculty of Medicine, Mansoura University.

In 2011, I got a scholarship from the Egyptian Government to do my MD study in Germany. In 2012, I started my MD thesis with the title "Identification of the molecular role of Pelota protein (PELO) by analysis of conditional Pelo-knockout mice." in the Institute of Human Genetics, University of Göttingen.

List of Publications

1. Varges D, Schulz-Schaeffer WJ, Wemheuer WM, Damman I, Schmitz M, Cramm M, Kallenberg K, Shirneshan K, **Elkenani M**, Markwort S, Faist M, Kohlhase J, Windl O, Zerr I (2013): Spongiform encephalopathy in siblings with no evidence of protease-resistant prion protein or a mutation in the prion protein gene.J Neurol 260, 1871-1879

2. Tan X, Xu X, **Elkenani M**, Smorag L, Zechner U, Nolte J, Engel W, Pantakani DV (2013): Zfp819, a novel KRAB-zinc finger protein, interacts with KAP1 and functions in genomic integrity maintenance of mouse embryonic stem cells. Stem Cell Res <u>11</u>, 1045-1059

3. Mohamed BA, Barakat AZ, Held T, **Elkenani M**, Mühlfeld C, Männer J, Adham IM (2014): Respiratory distress and early neonatal lethality in hspa4l/hspa4 double-mutant mice. Am J Respir Cell Mol Biol <u>50</u>, 817-824

4. Raju P, Nyamsuren G, **Elkenani M**, Kata A, Tsagaan E, Engel W, Adham IM (2015): Pelota mediates gonocyte maturation and maintenance of spermatogonial stem cells in mouse testes. Reproduction <u>149</u>, 213-221

5. **Elkenani M** , Nyamsuren, Raju P, Liakath-Ali K, Hamdaoui A, Kata A, Dressel R Klonisch T, Watt FM, Engel W, Pantakani DV, Adham IM. Pelota Regulates Epidermal Barrier Acquisition by Modulating BMP and PI3K/AKT Signaling Pathways. Manuscript submitted to International Journal of Investigative Dermatology. Under Review